GIMA
Geographical Information Management and Applications

Characterising housing stock vulnerability to floods by combining UAV, Mapillary and survey data - A case study for the Karonga district in Malawi

MSC thesis by Inez Gortzak

February 28, 2021

Universiteit Utrecht
TU Delft
University of Twente.
Wageningen UR
510
AN INITIATIVE OF THE NETHERLANDS RED CROSS

Characterising housing stock vulnerability to floods by combining UAV, Mapillary and survey data – A case study for the Karonga district in Malawi

Author: Inez Gortzak
E-mail: i.gortzak@students.uu.nl
Student number: 6923356

Master Thesis submitted to the joint venture of Utrecht University, TU Delft, Wageningen University & Research, University of Twente, in partial fulfilment of the requirements for the degree:

Master of Science in Geographic Information Management and Application

Supervisors:
Marc van den Homberg (510)
Maarten van Aalst (ICT)

Responsible professor:
Menno-Jan Kraak (ICT)

February 28, 2021

Preface

Before you lies the thesis *'Characterising housing stock vunerability to floods by combining UAV, Mapillary and survey data, a case study for Karonga, Malawi'*. This thesis has been written as part of the masters programme Geographical Information Management and Applications, in the period between September 2020 and February 2021. There have been some great people who guided and motivated me throughout this, extra challenging, period of research, that I would like to thank.

This research has been written in cooperation with 510, an initiative of the Netherlands Red Cross. 510 aims to use data analysis to improve the speed, quality and effectiveness of humanitarian aid. Marc van den Homberg, who supervised me from 510, helped me establishing the research topic and provided me with relevant datasets and literature. Our weekly meetings were always very helpful and gave me the motivation to continue. Maarten van Aalst, my supervisor from ICT, always provided me with great advice and feedback. I would like to thank the both of you for this inspiring cooperation. Jacopo Margutti and Christopher Beddow helped me during some technical challenges. I am grateful they were willing to invest some time to provide me with guidance.

Moreover, I am thankful to Mees Kraaijenbrink for his great help with excel and his continuous support, and to Tim Suijderhoud for reviewing parts of my thesis.

I hope you will enjoy reading this thesis.

Inez Gortzak

Abstract

To accurately identify the most vulnerable areas to floods, physical (e.g., building material) and social (e.g., education, health, income of households) housing stock information is required. However, in developing countries, this information is often unreliable, unavailable or inaccessible, and manual data collection is time-consuming. This can lead to difficulties for humanitarians or policymakers in implementing appropriate disaster risk reduction and response interventions. Therefore, there is a need for the development of alternative approaches to data collection and analysis. An alternative approach to on-site vulnerability assessment is to extract physical vulnerability characteristics, such as land use type or rooftop material, from satellite or Unmanned Aerial Vehicle (UAV) imagery. However, it is often not possible to extract other social or physical vulnerability information on the household level from solely from remote sensing data. This research develops an approach for integrating multiple data sources into a Geographic Information System to improve the completeness of data on different vulnerability indicators. This approach is applied to the housing stock of the Karonga district in Malawi. An Object-Based Image Analysis of UAV imagery is combined with a machine learning analysis of Mapillary data to enable remote identification of both rooftop ànd wall material. Depth-damage curves were created to describe the flood impact on the housing stock for different categories of physical vulnerability (such as building material) and levels of inundation. Moreover, local survey data is used for the creation of a social vulnerability index. Combined, the datasets represent the spatial distribution of housing stock vulnerability for multiple flood scenarios. This approach is useful in situations in which proactive risk analyses must be carried out or local-scale interventions, such as building strengthening- or flood awareness projects, have to be implemented. Finally, recommendations are given for scaling the methodology to areas where only lower resolution data is available.

Contents

List of Figures

List of Tables

Abbreviations

CNN Convolutional Neural Networks

DSM Digital Surface Model

DTM Digital Terrain Model

FbF Forcast based Finance

GIS Geographic Information System

GVH Group Village Headman

NDSI National Spatial Data Infrastructure

OBIA Object Based Image Analysis

OSM Open Street Map

SVI Social Vulnerability Index

SVM Support Vector Machine

TA Traditional Authority

UAV Unmanned Aerial Vehicle

VHR Very High Resolution

1 Introduction

1.1 Context

According to the United Nations Office for Disaster Risk Reduction (UNISDR, 2017) floods are the natural hazards with the highest frequency and the widest geographical distribution. In 2019 hazardous flood events resulted in approximately 40% of the worldwide deaths caused by natural disasters (World Resource Institute, 2020). With the effects of climate change and altering land use patterns, the number and intensity of floods have increased – and are anticipated to increase in the future (Nasiri et al., 2016). Flood risk reduction is therefore highly prioritised by organisations and governmental institutions. Aiming to improve disaster risk management by creating a better understanding of all dimensions of disaster risk – including vulnerability to floods -, the Sendai Framework for Risk Reduction was adopted in 2015. One of its priorities for action is to promote the use of reliable data and geographic information systems (GIS) to improve methodologies for risk and vulnerability assessment. The concept of vulnerability underlines the importance of physical and socio-economic factors that play a role in the impact of risks and that determine the resilience of communities (Birkmann, 2006). Hazard information can be combined with vulnerability information in order to predict who and what exactly will be exposed to a flood and what damages will occur (de Moel et al., 2015). Commonly, hazard and vulnerability maps are used to represent local flood situations, as they enable to give strong impressions of the spatial distribution of those factors (Merz et al., 2007).

Humanitarian organisations use flood risk and vulnerability assessment to predict the impact of future hazards and to formulate response strategies for risk reduction. The International Red Cross and Red Crescent Movement initiated Forecast-based Finance (FbF) with the aim of developing early warning systems to enable humanitarians to take action prior to the disaster (IFRC, 2020). With this shift towards pre-disaster strategies, humanitarian practices become more efficient and effective (De Perez et al., 2016).

1.2 Problem description

One of the areas in which the Red Cross aims to implement these strategies is the Karonga district in Northern-Malawi. This district is prone to sudden-onset floods, such as river and flash floods. Moreover, a large part of the Malawian population lives in poor quality informal housing, often providing insufficient protection during a flood event (UN-HABITAT, 2010). Disastrous flood events happen on a yearly basis, causing large economic damage in the housing sector and consequently in the displacement of thousands of people (Malawi Government, 2019).

An accurate object-based vulnerability map of the housing stock of Karonga could help in identifying the most critical areas prior to floods. However, one of the largest barriers with regard to flood-related early warning in developing countries - including Malawi, is the scarcity of reliable data on the household level (De Perez et al., 2016). In assessing the physical vulnerability to floods – the impact of a flood event on physical structures, information on building material, size and condition of buildings is essential. Cadastral information is often unavailable or inaccessible due to policy restrictions or high costs (Blanco-Vogt et al., 2013). In addition, as information varies from building to building, manual data collection would be a time-consuming process (Papathoma-Köhle, 2016). Common assessments are therefore mostly based on aggregated land use data that do not allow for differentiating between buildings within the same land use class. Research by Englhardt et al. (2019) and Wouters et al. (2020) aimed to solve the previously mentioned problems by identifying rooftop characteristics automatically. This was attempted by using remote sensing imagery and Object-Based Image Analysis (OBIA) techniques. Damage curves derived from literature were coupled to the rooftop material classes in determining the vulnerability of the buildings.

However, this approach is challenged by two different factors. Firstly, damage curves bring with them specific uncertainties in developing countries. Empirical damage data is scarce due to

limited data collection after a hazardous event, resulting in low availability of accurate damage data (Khalfan, 2013). Secondly, by basing physical vulnerability on assumptions related to rooftop material, only a limited part of the concept is covered. Other indicators such as wall material, the amount of windows/openings and the number of floors, play an important role as well (Tarbotton et al., 2015). In addition, indicators determining social vulnerability, such as income, education and health, are important to take into consideration (Birkmann, 2006; de Moel et al., 2015).

To indicate what areas are expected to be most vulnerable to floods, this research aims to construct an approach for accurate object-based vulnerability mapping of the housing stock in Karonga. This research builds upon the extensive data collection initiatives of the Malawi Red Cross in cooperation with 510. High resolution drone imagery, street-view imagery and household survey data have been collected after a flood event in March 2020. This dataset allows for the identification of both physical and social vulnerability indicators by using a remote approach. In this research, the data sources are combined to improve knowledge on flood vulnerability. Moreover

1.3 Structure

The remainder of this report is structured as follows. In Chapter 2 an overview of relevant concepts and theories within flood risk and vulnerability assessment is presented. Moreover, attention goes out to Object-Based Image Analysis, a commonly used method to remotely assess physical flood vulnerability. Based on these concepts, theories and methods, the scope and objectives of this research are narrowed down and formulated in Chapter 3. Chapter 4 entails an overview of the case study area, the input data and the methods that have been used to derive vulnerability information and to construct vulnerability maps. In Chapter 5 the results are presented. This chapter is structured according to the sub-questions of this research. Each sub-section discusses the findings in relation to a sub-question. In Chapter 6 results are discussed and the validity and limitations of the research approach are analysed. Lastly, in Chapter 7 the sub- and main questions are answered. Moreover, recommendations are made for future research.

2 Theoretical Background

This chapter provides a theoretical background of the previously described context and problem statement. It starts by introducing flood risk and vulnerability concepts such as commonly used assessment methods, damage curves and the importance of scale. Then, it describes a commonly used method for the identification of vulnerability attributes based on a remote approach. Finally, some important implications and conclusions for this research are given.

2.1 Flood risk and vulnerability assessment

Within the science of natural disasters, risk refers to the probability that natural events of a given magnitude and a given loss will occur (Merz et al., 2007). Whereas in the past natural disasters were mostly seen as physical occurrences, today a more holistic approach is used to describe, assess and predict disasters. Birkmann (2006) defines disasters as "*the result of complex interactions between a potentially damaging physical event (e.g. flood, earthquakes, tsunami) and the vulnerability of a society, its infrastructure, economy and environment, which are determined by human behaviour*". The nature of a risk is thus not only determined by the physical hazardous event, but also by the exposure and vulnerability of the elements at risk (IPCC, 2012; Merz et al., 2014; UNDRR, 2019). By integrating the vulnerability concept, the risk definition is broadened by recognising risk as a human subject instead of a completely environmental or technocratic subject – groups are not only at risk because they are exposed to a flood or earthquake, but also because of their socio-economic status, access to resources and livelihood context.

In flood risk assessment information models from various disciplines are combined with the goal to estimate the probability and severity of floods (de Moel et al., 2015). Risk assessment can take many forms, ranging from qualitative household surveys to remote sensing analysis. However, the main components for evaluation in risk assessment are hazard, exposure and vulnerability (Merz et al., 2007). The extent of flood damage depends not only on the flood characteristics but also on the vulnerability of the inundated area, meaning that a higher vulnerability of people and buildings leads to higher flood damage. The interplay between the concepts is therefore used to predict flood risk.

An important component of risk assessment is damage assessment. Damage estimations can assist policymakers in choosing practices for risk mitigation and in allocating resources for disaster response (Wouters et al., 2020). Flood damage assessment is commonly used in combination with GIS methods for risk mapping to illustrate the spatial distribution of damage within an area.

Merz et al. (2007) describe the workflow for flood damage assessment in relation to GIS and mapping, visualised in figure 1. Here, flood hazard is characterised by its probability of occurrence and intensity. Factors such as inundation depth, flow velocity, duration and rate of water rise determine the severity of the hazard. The values of the factors may differ over a certain area and flood hazard maps are used to show the spatial distribution of the hazard. The vulnerability of an area is determined by the exposure and susceptibility of all elements - e.g. people, buildings, infrastructure, ecosystems - located in the area. Exposure refers to the number of elements that are be affected by the flood. In case of figure 1, the red buildings, its inhabitants and their property are exposed by the flood, depending on the water depth. The loss that will occur depends on the susceptibility of the exposed elements, which can be determined by damage curves. Together, exposure and susceptibility information are used to represent the building vulnerability of an area. When both a hazard and vulnerability map are combined, the actual spatial distribution of flood risk can be visualised.

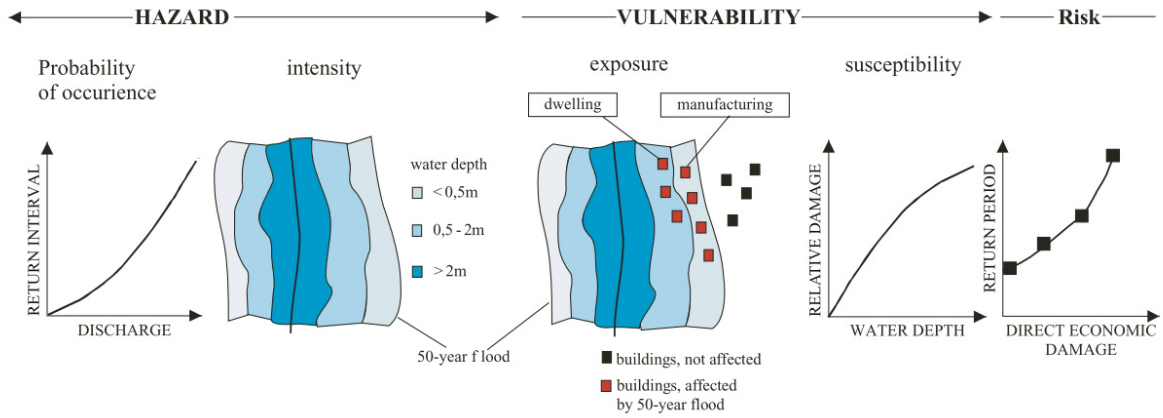

Figure 1: The interplay between hazard and vulnerability for estimating flood risk (Merz et al., 2007)

Within flood vulnerability analysis a distinction between social and physical vulnerability can be made. Whereas social vulnerability relates to the susceptibility of and impact on social groups, does physical vulnerability represent the same features for structural elements (Birkmann, 2006; Guillard-Gonçalves & Zêzere, 2018). The indicators that are used to assess social vulnerability are generally hazard-independent, for example, education, income, age, gender, health/disability (Schneiderbauer & Ehrlich, 2006). Health largely determines an individual's ability of coping with a natural hazard and education plays an important role in acquiring flood-related knowledge. Indicators for measuring physical vulnerability are often hazard-dependent as they represent the physical damage on exposed elements as a result from a certain flood event. Indicators that determine building stability such as quality, building material, age and size are often taken into consideration (Schneiderbauer & Ehrlich, 2006). However social and physical vulnerability are not inseparable. Physical vulnerability can be seen as an expression of social vulnerability as, for example, people with disabilities or a lack of education generally have less opportunity of buying a good quality house in a low-risk area. Birkmann (2006) and Guillard-Gonçalves and Zêzere (2018) therefore state that it is important to use a balanced approach between social and physical indicators in vulnerability assessment in order to represent the vulnerability concept as a whole.

2.1.1 Damage curves

As previously mentioned, a commonly used approach to identify the susceptibility of exposed buildings is by assessing the potential damage on the housing stock based on depth-damage curves. Depth-damage curves quantify flood vulnerability by relating water depth at the affected object to a damage grade (de Moel et al., 2015; Merz et al., 2014). It is important to use separate functions for different building material types, as, for example, a mud house will collapse at a lower water depth compared to a brick house (Wright, 2015). Damage curves can be developed based on an empirical or synthetic approach (Merz et al., 2010). Empirical damage curves are developed with damage data collected after flood events. Damage data is often collected in databases with the aim to harmonise the data and to make it easily accessible (Kellermann et al., 2020). Examples of databases are the German HOWAS, in which object-specific flood damage data of Germany is collected.

The synthetic approach is based on aspects as land cover, object type, survey information or what-if-questions. The expected damage is then estimated for certain flood situations (Merz et al., 2010; Wouters et al., 2020). An example of a what-if question could be: what damage would you expect if the water depth was 1.5 meters above the floor of a wooden building?

In developed countries empirical damage curves based on extensive damage databases are commonly used by insurance companies for the estimation of damage costs (Kellermann et al., 2020).

However, determining the curves remains a challenge due the fact that they are mostly based on a limited amount of measurements or studies. The quality of damage curves can therefore be poor or difficulties arise when curves are transferred to other contexts (Merz et al., 2010). Those challenges play even a larger role in developing countries, where data collection after a hazardous event is scarce. This results in low availability of accurate damage curves for building materials of houses in developing countries and can thus result in unreliable risk calculations (Khalfan, 2013).

In cases where empirical databases are unavailable or inapplicable, the synthetic approach can be used. Rudari et al. (2016) used the synthetic approach in the context of Malawi. They classified the building typologies in the case study area according to the classes: 1) traditional, 2) semi-permanent and 3) permanent. Curves were derived from the CAPRA library, based on the building materials present in the research area. The curves were then aggregated according to the materials belonging to the classes. A similar method was used by Wouters et al. (2020).

2.1.2 Scale and up-scaling

Wu and Li (2006) define scale as the spatial or temporal dimension of a phenomenon and scaling as the transfer of information between scales. Those concepts play an important role in risk and vulnerability assessment. The interdisciplinary relation between patterns and processes of risk operate on different spatial and temporal scales. Moreover, a match between the scale of the risk, the policy level and the scale of the available data is essential in accurately assessing the risk and in determining suitable measures (Kienberger et al., 2013).

Merz et al. (2010) divide flood damage assessment into the micro-, meso-and macro-scale. de Moel et al. (2015) add the supra-national-scale to this array. On the micro- or local-scale, assessments are based on single elements at risk. Detailed information about buildings, infrastructure or terrain elevation of a certain community can be incorporated. Such detailed assessments can support the development of local flood measures or urban planning strategies. Meso- or regional-scale assessments are based on spatial aggregations such as residential areas, river basins, administrative units or zip code areas. In the context of floods, meso-scale assessments are very valuable as they allow for the identification of flood risk and vulnerability in a certain catchment. Macro-scale assessments are based on larger spatially aggregated units, such as municipalities, regions or countries. For instance, many European countries have developed flood models for main cities or vulnerable areas. Damage is often calculated by relating land use classes to damage curves. Another method is to combine meso- or micro-scale assessments and aggregate them to the national level. However, this raises problems as the different methods used in local scale assessment makes the output difficult to compare. At the supra-national-scale, risk or vulnerability is estimated for areas such as Europe. Those assessments are generally less detailed and represent a more generalised picture of the situation.

The scale of assessment depends on the level of policy intervention that is wished for (Lang et al., 2014). Although assessment on the micro-scale might reveal the highest level of detail, if policy measures will be implemented on the regional-scale, aggregated information will be used instead of individual-based information. On the other hand, if local measures for floods are taken, policy makers have to take into account that the down-scaling of a national flood vulnerability map does not result in an accurate representation of the local situation (Kienberger et al., 2013). This relates to figure 2 in which the relation between scale, complexity and aggregation is depicted. Kienberger et al. (2013) state that, in general, it can be observed that the spatial and time variability of vulnerability increases when looking at the individual and is more generalised towards the more aggregated assessments. Depending on the level of complexity of the information that is required, the level of aggregation can be determined upon.

Moreover, the decision on spatial scale is interlinked with the availability and resolution of data. High resolution data is essential in assessing vulnerability on the building level, whereas aggregated land use data suffices for national-level assessments.

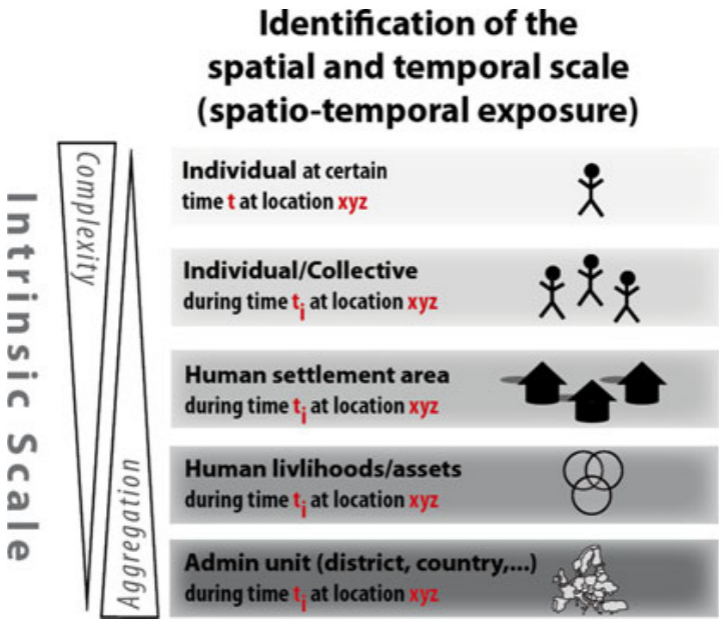

Figure 2: The relation between complexity, aggregation and spatio-temporal scale (Kienberger et al., 2013)

Lang et al. (2014) use the 'geon' approach to represent spatial patterns at different scales. They define a geon as "*a region that is delineated based on uniform response to a phenomenon under space-related concern*". By classifying an area into geons, multiple indicators are used to identify spatial patterns throughout an area. Clusters are formed if homogeneous characteristics can be observed. The division of geons goes beyond formal borders and can help to comprehend the spatial distribution of phenomena. Lang et al. (2014) exemplify this by referring to segmentation in Object Based Image Analysis (see section 3.2). Areas that share similar texture, colour, shape or spectral signature, are formed into a cluster. However, other indicators can be used as well. Kienberger (2012) used the geon approach for modelling flood vulnerability in Mozambique. Within the spatial extent of a flood, a group of geons represented the spatial distribution of vulnerability, with the aim to support decision-makers in getting an overview of vulnerability hot spots.

Based on the required indicators and the required level of policy support, geons can be aggregated or scaled-up into larger spatially homogeneous areas. Kienberger (2012) used this approach to scale-up from the community level to the district level.

2.2 Remote sensing and Object-Based Image Analysis

One of the largest challenges for measuring exposure and physical flood vulnerability in developing countries is the characterisation of the built environment, due to the absence of accurate cadastral data (Blanco-Vogt et al., 2013). However, with the increase of Very High Resolution (VHR) satellite and drone data, remote sensing-based techniques (e.g. image classification, object detection) are increasingly becoming a time-saving alternative to cadastral field surveys. The classification process of VHR imagery is usually done through Object Based Image Analysis (OBIA) methods. OBIA methods involve grouping pixels into objects based on their spectral properties (Blaschke, 2010).

OBIA broadly exists out of two parts: 1) image segmentation and 2) feature extraction and classification. Image segmentation is the process of clustering pixels of an image into homogeneous and meaningful areas. (Blaschke, 2010). Segments are vector shaped and share criteria such as texture, colour, shape and size. Many algorithms that automatise the segmentation process have been developed throughout the years in remote sensing applications.

Spatial resolution and scale play an important role during the segmentation process. Segments can only be formed on meaningful objects if the pixel size of the image is small enough. For images with a coarse scale only large features, e.g. forest or agricultural areas, can be identified, whereas images with a finer scale allow for the identification of individual plants and trees (Blaschke, 2010). The parameter and threshold values of the algorithm should therefore be tuned according to the resolution of the image and the preferred outcome. There are no general rules for the relationship between spatial resolution and parameter values, and value selection is dependent on trial-and-error (Grippa et al., 2016).

The classification step is based on machine learning algorithms that use training and validation samples as input. Those samples contain land use classifications and spectral features (e.g. maximum, minimum, mean and standard deviation of the spectral bands). The algorithm is trained to classify the segmented image based on the features derived from the training samples (Wouters et al., 2020). Maximum likelihood Classifier (MLC), decision tree (DT), K nearest neighbour (KNN) and Support Vector Machine (SVM) are frequently used machine learning algorithms for classification. However, SVM is often seen as the best performing one for land use classification (Grippa et al., 2016; Qian et al., 2015).

OBIA has been widely explored for the classification of land use and building and damage detection. However, only a few studies aimed to apply OBIA for the classification of buildings in the context of vulnerability assessment. Ebert et al. (2009) applied OBIA for the estimation of variables that determine social vulnerability in the context of risk management. They, for example, used optical, LiDAR and elevation data to delineate buildings and to determine building vulnerability based on surface slope. Blanco-Vogt et al. (2013) propose a method for the clustering of buildings with similar typologies based on parameters that can be estimated with remote sensing. They distinguish between six parameters: 1) height, 2) size, 3) form, 4) roof structure, 5 and 6) topological relation to neighbours and open space. De Angeli et al. (2016) used the previously mentioned parameters for developing a flood damage model in urban areas. The parameters were used to represent a higher level of variability compared to aggregated land use classes, leading to higher detail in vulnerability levels. Research by Englhardt et al. (2019) was conducted with a similar aim and made use of detailed building construction characteristics to distinct between physical vulnerability in rural and urban areas.

However, OBIA techniques are limited to the identification of buildings from a nadir perspective and do not allow for the integration of street-level details such as wall material (Cao et al., 2018). In order to decrease the amount of uncertainty that comes with satellite and drone data, Wouters et al. (2020) therefore suggests that additional data sources, such as street view data should be incorporated in vulnerability assessment as well. Cao et al. (2018) and Hoffmann et al. (2019) have showed the potential of fusing information derived from street-view data with nadir-view data, based on deep learning Convolutional Neural Networks (CNN). In both researches was concluded that street-level data can provide details that largely improve land use classifications solely based on VHR data.

2.3 Implications for this research

Based on the previous described theories, the following conclusions and implications for this research can be drawn. First of all, the vulnerability concept plays an important role in determining flood risk. An investigation of this concept in the context of Malawi can result in new flood-related insights from a human-centred perspective. To identify the physical vulnerability of buildings, the susceptibility of building materials can be related to depth-damage curves. Depth-damage curves are usually developed for different material types, but are of limited quality and availability in developing countries. In the case of Malawi, a synthetic damage curve approach, related to the methodology of (Rudari et al., 2016), would be a good alternative.

OBIA techniques on satellite or drone data are promising in determining vulnerability indicators from an oblique perspective, such as rooftop structure, height and size. This offers a good alternative to field surveying in areas where cadastral data is unavailable or inaccurate, which is the case in Malawi. However, OBIA is challenged by the fact that it only allows for the identification of a part of the indicators. Additional data sources are required to identify street-level indicators such as wall material and openings. Deep-learning models based on CNN allow for the automatic recognition of indicators from street-view imagery. The combination of indicators derived from both data sources would thus result in a higher level of detail in identifying physical vulnerability. In addition, as stated by Birkmann (2006) and Guillard-Gonçalves and Zêzere (2018) physical vulnerability indicators should be further enriched by social vulnerability indicators to get an overview of the concept as a whole.

Kienberger et al. (2013) and Lang et al. (2014) mention that the match between the scale of assessment, data and policy intervention is indispensable in risk management. As a result of extensive data collection of the Red Cross in settlements in the Karonga district, assessment at the individual level is possible. However, in other areas a limited collection of data can result in lower complexity and higher aggregation of the assessment outcomes. It is therefore important to see what can be learned from local scale assessment and how the local methods can be applied on other scales. Moreover, a bridge between areas of higher and lower data availability should be build to get an overview of the possibilities for vulnerability assessment at multiple scales.

3 Objective and research questions

This chapter presents the objective of this research and the corresponding research questions. Moreover, the scope and the hypothesis are discussed.

3.1 Research objective

The objective of this research is to gain understanding of the physical flood vulnerability of buildings in the Karonga district by using a remote approach to the identification of building material. Furthermore, the correlation with social vulnerability is assessed. An approach is developed for the integration of data sources of multiple types (UAV, Mapillary and survey data) to increase the number of vulnerability attributes and to improve the completeness of vulnerability assessment on a local scale. Material-based damage curves are improved as well as adapted to the context of Karonga by including local damage data. Moreover, to analyse the applicability of this assessment method to other scales and contexts, a framework is developed for up-scaling in relation to data availability and intervention scale.

The improved knowledge on flood vulnerability can be used to assess vulnerability in more detail, allowing for improved decision-making tools used in the development of Disaster Risk Reduction strategies. Moreover, an enhanced understanding of the local vulnerability situation can play a crucial role in identifying the most critical areas for humanitarian response interventions.

3.2 Research questions

Based on these objectives, the following research question is formulated:

In what way can UAV, Mapillary and household survey data be combined in order to assess housing stock vulnerability to floods in Karonga, Malawi?

The following sub-questions will be answered in order to formulate an answer to the research question:

- **SQ 1** What physical and social vulnerability attributes can be derived from the acquired datasets?
- **SQ 2** How can local damage data be used to improve flood damage curves for Karonga?
- **SQ 3** To what extent do additional data sources add to the completeness of housing stock vulnerability attributes?
- **SQ 4** To what extent are the methodology and results of this micro scale study applicable to other scales

Figure 3 shows the different research steps with corresponding methodology that lead to answers to the sub-questions and consequently to an answer to the main question. The first question is based on identifying building material from UAV, street-level and survey data. The methodology is based on Wouters et al. (2020) and on a model created by 510. Secondly, the results of this analysis were used to improve existing flood damage curves, derived from the CAPRA library. then, it is analysed how the datasets can be combined and what the added value of the combinations are for vulnerability assessment. Patterns in building material and vulnerability were identified with the aim to predict flood vulnerability in other, more data scarce areas as well. Moreover, recommendations are given for scaling to other areas. Ultimately, the answers to all sub-questions together form the answer to the main question.

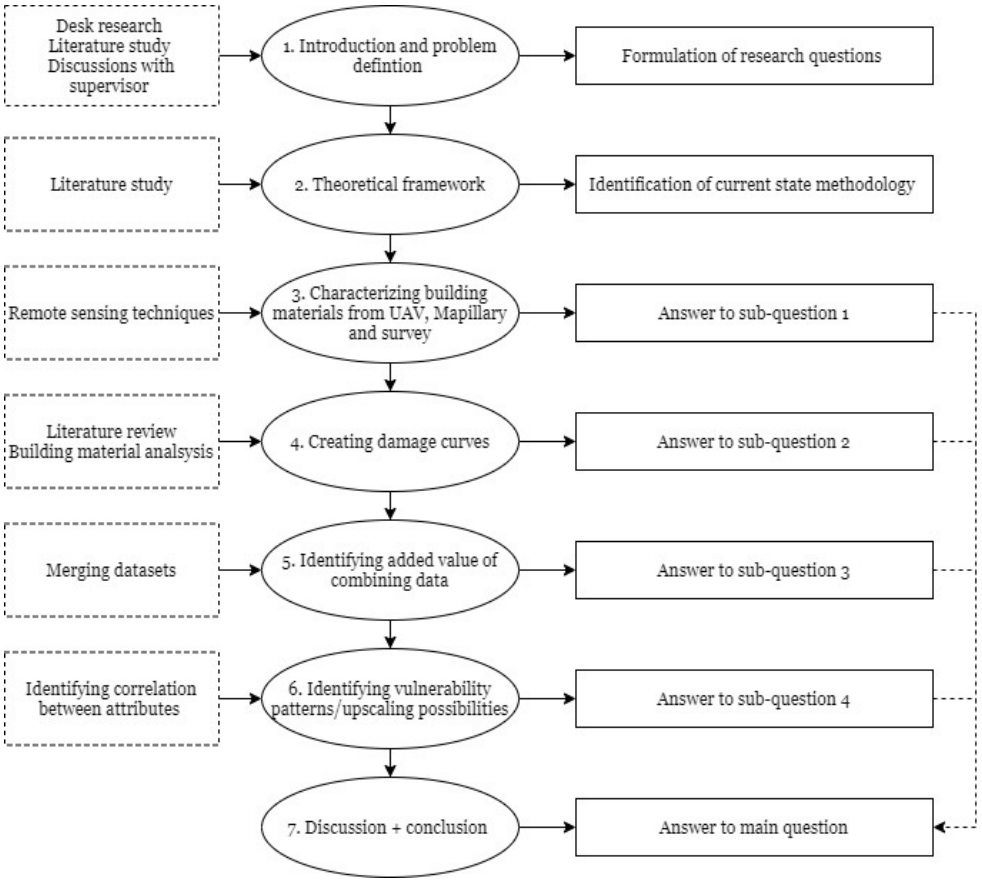

Figure 3: Conceptual framework of research steps, questions and methodology

3.3 Scope

This research focuses on identifying how UAV, street view and household survey data can be adequately combined to improve housing stock vulnerability assessment in the Karonga district. The methodology used to identify rooftop material with UAV is based on research by Wouters et al. (2020) and the model used to recognise wall material from street-view imagery is developed by 510. It must be noted that it is not intended to adapt or fine-tune the previous mentioned methodology and model. It is aimed to combine both to get a higher level of detail in physical vulnerability assessment. Moreover, this research explores the possibilities with regard to up-scaling to other areas. The goal is not to create vulnerability maps for the entire country of Malawi, but to create an overview of different levels of aggregation in data, complexity and corresponding policy and intervention levels that can be reached with the presented approach.

3.4 Hypothesis

The hypothesis of this research is that drone and Mapillary data are promising information sources to remotely identify building characteristics in data poor areas. Data on building characteristics can be used to assess the physical vulnerability to floods by linking building material to damage curves. It is expected that the accuracy of vulnerability assessment will improve when UAV data is combined with street view data. This hypothesis will be tested in a small area in the Karonga district in Malawi. In addition, it is expected that an adapted version of the methods used for this small scale assessment can be applied on a larger scale. For example, the relationships between wall and rooftop material in the research area can be related to other areas with a similar housing stock for to identify vulnerable areas. Instead of UAV data, the application of satellite and census data might be good alternatives on a larger scale.

4 Methodology

This section describes the methodologies that have been used in this thesis. Multiple data sources are combined for the identification of building characteristics and therefore different methodological approaches have been used. Moreover, the different outputs were combined and linked to damage curves in order to assess the vulnerability of the buildings. This step requires an additional methodology which has been explored in this thesis. This section starts by introducing the case study area of the research, followed by a description of the input data, the methods and the software that were used.

4.1 Case study area

Malawi is a landlocked country in the South-Eastern part of the African continent. The country is bordered by Lake Malawi and by the countries Mozambique, Tanzania and Zambia. Figure 7 shows the location of Malawi. In 2018 a Population and Housing Census report was published by the Malawian National Statistical Office. In this report was stated that the country has a population of 17,5 million people with an average annual population growth rate of 2.9%. The largest part of the population lives in rural villages. Due to its sub-tropical climate and location, Malawi is prone to natural disasters such as heavy rain, floods and earthquakes.

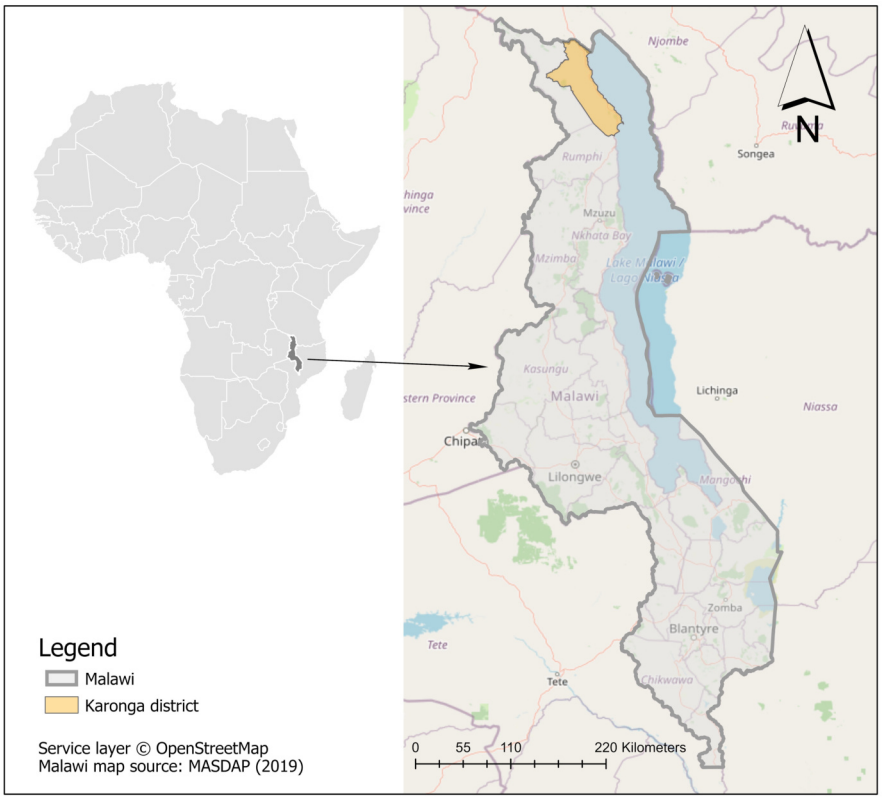

Figure 4: Location of Malawi and the Karonga district

Heavy rainfall in January 2015 caused extensive floods which affected more than 1 million people, left 230.000 displaced and killed more than 100 (Malawi Government, 2015). In March 2019, Malawi experienced another severe flood, with again devastating consequences. The quality of the building construction has a crucial influence on the impact of natural hazards on the society. Yet, after the 2019 floods the largest economic damage was perceived in the housing sector, leaving Malawi's society extremely vulnerable (Malawi Government, 2019). A study by UN-HABITAT (2010) shows that 20% of Malawi's housing stock in urban areas is considered as formal and in rural areas this only counts for 5%. Moreover, it is estimated that only 1% of the population can afford housing by the formal private construction sector. The majority of

the Malawians live in informal settlements in either formally planned Traditional Housing Areas (THAs) or in informal neighbourhoods – both in which basic services are limited or missing. Protection against natural disasters is extremely low in these areas as a result of: '1) poor quality of construction materials, 2) poor construction practice due to a lack of skilled labour, and 3) lack of building design and construction provision for natural disasters' (Kloukinas et al., 2020). After the flood in 2019, the government therefore decided to improve its disaster risk management strategy by "building back better". The strategy includes promoting resilience by adopting hazard-resistant construction standards, improving the physical planning system and strengthen flood-forecasting and prevention systems (Malawi Government, 2019).

This research will focus on settlements in the Karonga district, located in the northern part of Malawi (see figure 7). The district is characterised by large differences in relief between the mountainous area in the western part and the lake shore in the eastern part, leaving the lower areas vulnerable for floods (Bucherie, 2019). During the floods in 2014, the Karonga district was one of the most affected areas in Malawi (Malawi Government, 2015). Previous research by Bucherie (2019) pointed out that the district is not only prone to riverine floods, but also to flash floods – events caused by rapid runoff generation in combination with the sudden rise of water levels in the river banks. Therefore, multiple humanitarian organisations, triggered by the Humanitarian Aid department of the European Commission (ECHO), took action by implementing projects for developing early warning systems to increase resilience.

The housing stock of Karonga can be divided into three categories according to structural permanence (UN-HABITAT, 2010):

1. Permanent: roofs constructed with iron sheets, tiles, concrete and walls of burnt bricks, concrete or stones
2. Semi-permanent: a mix of permanent and traditional materials. Generally misses permanent construction materials for wall or roof
3. Traditional: thatched roofs and mud walls or walls made of mud and wattle

Table 1 shows the division of housing units and population over the previously mentioned building classes. Figures 5-7 illustrate the different building types. The pictures were taken during the ECHO 3 household survey in Karonga.

	Permanent	**Semi-permanent**	**Traditional**
Housing units	67,1%	18,5%	19,7%
Population	66,1%	18,4%	15,5%

Table 1: Ratio of housing units and population per building category in Karonga (UN-HABITAT, 2010)

Figure 5: Traditional house (MRCS, 2020)

Figure 6: Semi-permanent house (MRCS, 2020)

Figure 7: Permanent house (MRCS, 2020)

4.2 Input data

This research used five different data sources of the Karonga district as summarised in table 2. The majority of the data was collected by the Malawian Red Cross data team in collaboration with 510. The data was collected as part of the ECHO 3 project in Malawi, with the goal of strengthening resilience in urban an rural areas. The different datasets and their implementation purpose are discussed below.

UAV imagery

UAV imagery of the Karonga district was collected in May 2020 by the Malawian Red Cross in cooperation with 510. The data has a spatial resolution of around 0.11 meters and is therefore suitable for the identification of detailed characteristics in the landscape. This dataset was used to identify rooftop characteristics in the Karonga area. Based on the point cloud data that comes with the UAV imagery, a Digital Terrain Model (DTM) and Digital Surface Model (DSM) were constructed. The DTM represents the elevation of the bare ground of the research area and the DSM represents the elevation of the area including objects. Together, the DTM and DSM were used to estimate the building height.

Mapillary imagery

Mapillary is an open source platform that facilitates the collection of street view images based on crowd sourcing. Unlike Google Street view, Mapillary allows all contributors to upload street-level images that they can capture themselves by cameras or smartphones. Recently, the Malawian Red Cross captured an area of the Karonga district on Mapillary which partly overlaps with the household survey and UAV data. This dataset was used for identifying wall materials.

Household survey ECHO 3

A household survey was done in March 2020 to assess the aftermath of a flood disaster in February 2020. 916 households in Traditional Authorities Mwakaboko participated in the survey. The aim of the survey was to understand the magnitude of the flood by verifying the number of affected households in the affected areas. Information about building material, flood height and damage can be find in the corresponding table. Furthermore, the coordinates of the households were taken during the survey, allowing to add the information on a map.

The information of the survey was used for multiple ends. First, the survey provides insight in the water height and building damage. This information was used to adapt and improve CAPRA vulnerability curves to the context of Karonga. Second, the information was used as a validation source for the automated classification of rooftop material.

Household survey UBR

The Unified Beneficiary Registry is a Malawian initiative with the aim to integrate data from different social protection programmes. Through the registry, data from a household survey in the Traditional Authorities of Kilipula and Mwakaboko could be acquired. The dataset contains information about socio-economic factors, such as age, gender, household size and wealth. This information was used to generate the Social Vulnerability Index.

OpenStreetMap building layer

Open Street Map (OSM) is an open source mapping platform, that enables everyone to openly access and add data to the map. Commonly, mapathons are organised by OSM to communally map the objects of a certain area. In December 2020 the building layer of Karonga was updated during an online mapathon. During this event, the building footprint in the research area was manually delineated by using Maxar satellite data (captured in 2018) as reference data. The layer was used as a base layer to align all vulnerability attributes.

Dataset	**Data type**	**Implementation**	**Source**
UAV	Optical (+/- 0.11 m resolution)	Identifying rooftop material	MRCS/510 (2020)
UAV	DTM & DSM	Identifying building height	MRCS/510 (2020)
Mapillary	Street-level imagery	Identifying wall material	Mapillary (2020)
Household survey ECHO 3	Tabular (with coordinates)	Damage data/ validation	MRCS/510 (2020)
Household survey UBR	Tabular (with coordinates)	Social vulnerability indicators	UBR (2018)
OpenStreetMap Building layer	Vector shape file	Building alignment layer	OSM (2020)

Table 2: Overview of the required datasets

4.3 Methods and software

Figure 8 gives a broad overview of the workflow that was used in this research and table 3 lists the software tools that were used. First, the required vulnerability indicators or attributes were chosen. Then, the data was processed to acquire the vulnerability attributes. CAPRA damage curves were adapted according damage information derived from survey data. The vulnerability attributes were all fused into the OSM building layer to enable to accurately overlay them and to create a multi-attribute vulnerability map for Karonga. The damage curves were linked to the data layers containing building material types to get insight in the damage ratio per building for multiple flood scenarios. Based on the findings, recommendations were done for up-scaling of the methodology.

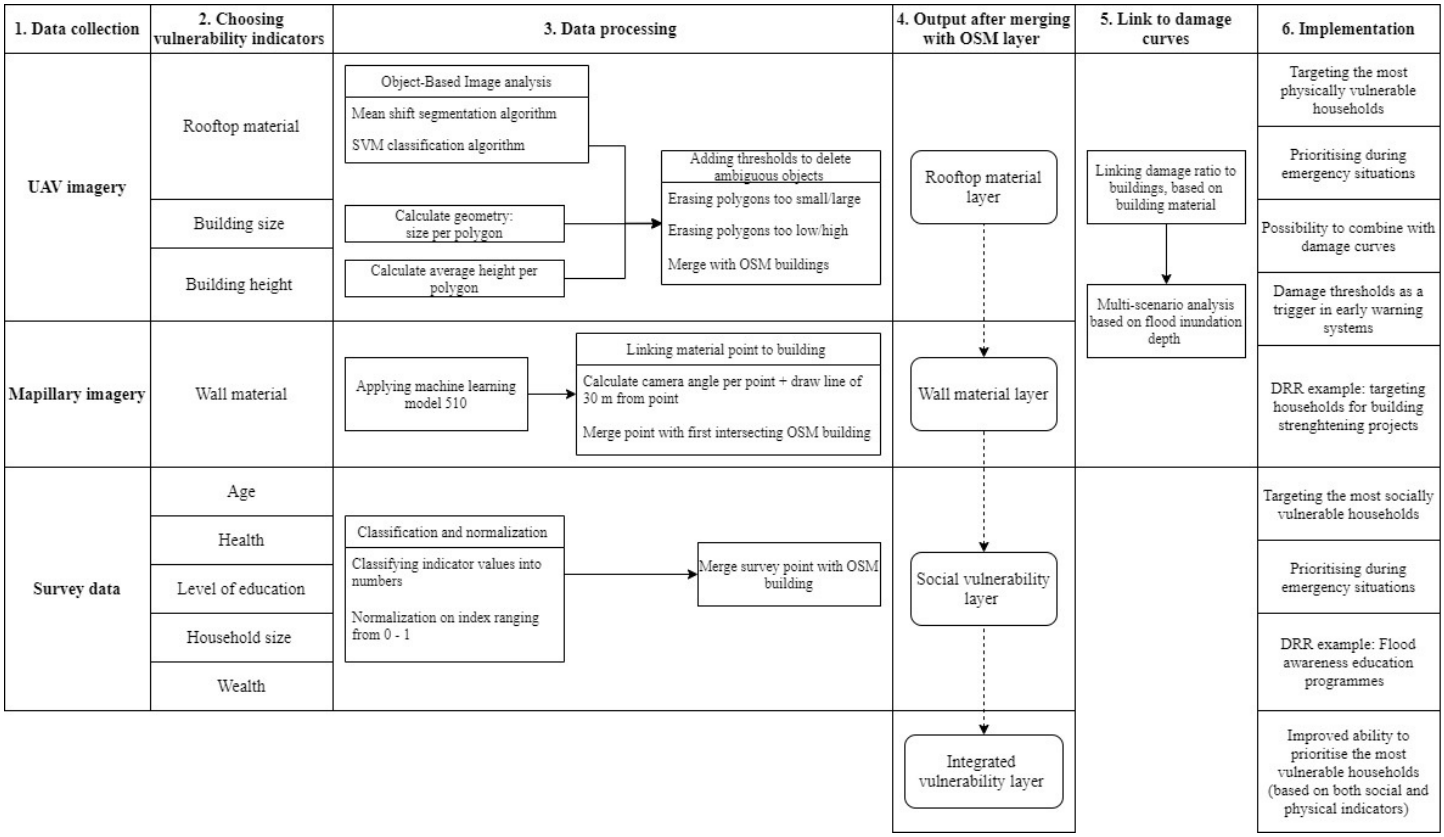

Figure 8: Model summary and usability per dataset

Software	Function	Implementation
ArcGIS Pro	Licence-based GIS software	Data visualisation
QGIS	Open-source GIS software	Remote sensing, merging data, visualisation
Orfeo Toolbox	Open-source remote sensing tool	Algorithms for OBIA
CAPRA	Risk assessment platform	Acquire damage curves
SPSS	Statistical software	Calculating correlations

Table 3: Software overview

The methodology for this research can be divided into four main steps that will be elaborated in the following sections:

1. Deriving vulnerability attributes from the datasets
2. Adjusting CAPRA vulnerability curves to the Karonga context and link to building material
3. Fusing data layers of vulnerability attributes in OSM building layer
4. Identifying patterns and clusters for up-scaling/doing recommendations for up-scaling

4.3.1 Deriving vulnerability attributes from the datasets

The first methodological step was to derive vulnerability information from the datasets. The previously mentioned data sources all allow for the identification of specific vulnerability attributes that are each implemented for a certain purpose. Table 4 summarises the vulnerability attributes that were derived from the UAV, Mapillary and survey data, together with the implementation purpose. The following sub-sections describe the methodological aspects of attribute identification from UAV, Mapillary and survey data.

Dataset	Vulnerability attribute	Implementation
UAV	Rooftop material	Physical vulnerability
	Building height	
	Building size	
Mapillary	Wall material	
Household survey (ECHO 3)	Building type	Validation
	Wall/rooftop material	
	Flood height	Improving damage curves
	Flood damage	
Household survey (UBR)	Age	Social vulnerability
	Level of education	
	Household size	
	Wealth	
	Fit for work	

Table 4: The vulnerability attributes that can be derived from the datasets and their implementation purpose

UAV

Deriving vulnerability information from UAV imagery was done by following the method of Wouters et al. (2020). Wouters et al. (2020) conducted an Object-Based Image Analysis with algorithms that were retrieved from the Orfeo Toolbox, an open source remote sensing tool and plug-in in QGIS. The workflow for OBIA is visualised in figure 9. The main goal of this research step was to differentiate between iron and thatched roofs, the two material types that are present in the research area.

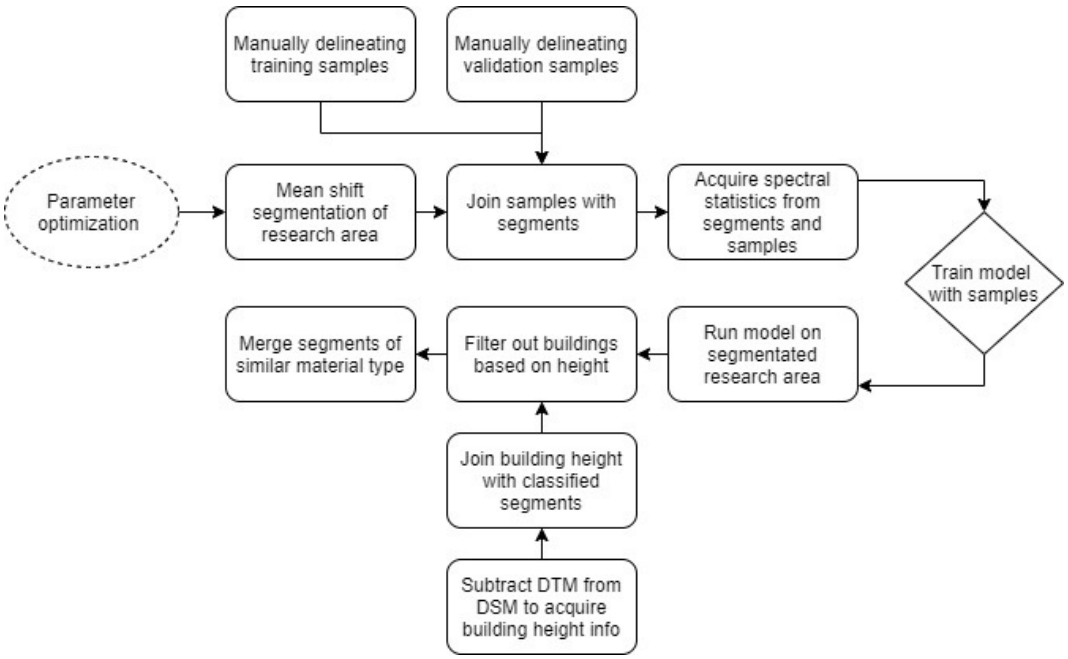

Figure 9: Conceptual model of automatic rooftop classification steps

First, training and validation samples were collected by manually delineating polygons of different land use types that were the most present in the research area. The samples were manually labelled according to the five land use types in table 5 and the spectral statistics were calculated. Table 5 shows the different labels that were given to the training samples, together with the mean values of the spectral bands. In addition, 200 validation samples (40 per class) were manually delineated and labelled according to the same classification scheme as the training samples.

Value	Label	Samples	Mean B0	Mean B1	Mean B2
1	Bare	25	208-251	183-240	156-229
2	Iron	28	114-255	208-255	185-255
3	Shadow	16	75-140	86-132	85-137
4	Thatch	44	175-248	155-240	145-234
5	Vegetation	15	130-196	159-217	126-167

Table 5: Training samples used to train the classification model

Then the mean-shift segmentation algorithm was used to automatically divide the UAV image into vector shaped objects based on their spectral properties. As previously mentioned, the parameter settings of the segmentation algorithm largely determine the outcome of the segments. To determine the correct parameter values, the algorithm was executed multiple times on a small area, by adjusting the parameter values after each run. Eventually, the best results were obtained with a spatial radius of 20 meter, a range radius of 15 (expressed in radiometry unit) and a minimum segment size of 80 (expressed in pixel unit). A relatively high value for the minimum segment size was chosen, to limit the number of polygons which allowed for faster computation times. Lastly, the spectral statistics were calculated for each segment to use as input for the image classification.

The classification model was trained by using the training and validation samples as input in the Support Vector Machine (SVM) algorithm. Consequently, the model was executed on the segmented research area to automatically classify the segments into land use classes. To make sure that segments labelled as iron or thatch really represent buildings, a height threshold was added. The height of the buildings was calculated by subtracting the mean height of the DSM of each building by the mean height of the DTM. The resulting value represents the building height. For buildings with a thatched roof a minimum height threshold of 0,5 meter and a maximum height threshold of 4,0 meter was added. For buildings with an iron roof a minimum height threshold of 0,7 meter and a maximum height threshold of 7,0 meter was added. This decision was made based on the fact that buildings of thatched roofs are generally lower compared to buildings with iron roofs. Moreover, the size of each polygon was calculated and a size threshold was added to erase polygons that did not represent buildings.

Accuracy assessment OBIA

To assess the quality of the automated land use classification, several statistics were calculated. The classified rooftops were compared to ground truth samples derived from the ECHO 3 survey to assess the accuracy of the classification. A confusion matrix was created in which the True Positive (TP), False Positive (FP), True Negative (TN) and False Negative (FN) classifications were listed. A commonly used statistic is the overall accuracy. This statistic divides the number of correctly predicted cases by the total amount of cases:

$$Accuracy = \frac{TP + TN}{TP + TN + FP + FN} \tag{1}$$

However, this statistic does not take into account unevenly distributed classes and can therefore give a distorted view on the quality of the model. To measure the quality of each separate classifier, F1-score was calculated. F1-score is determined by Precision and Recall. Where

Precision represents the ratio of the correctly classified positive cases to the total number of positive cases in that class. Recall represents the ratio of correctly predicted cases to all cases in that class (Wouters et al., 2020):

$$Precision = \frac{TP}{TP + FP} \tag{2}$$

$$Recall = \frac{TP}{TP + FN} \tag{3}$$

The F1-score represents the weighted average of Precision and Recall and thus incorporates both the False Positives and False Negatives. Moreover, this statistic is suitable when the number of cases are unevenly distributed over the classes, which is the case in this study.

$$F1 - Score = 2 * \frac{Precision * Recall}{Precision + Recall} \tag{4}$$

Lastly, the Cohen Kappa statistic measures the inter-observer agreement of classifiers. This statistic measures how well the the machine learning classifier matches the ground truth data, controlling for the accuracy of a random classifier (p_a).

$$\kappa = \frac{A - p_a}{1 - A} \tag{5}$$

Mapillary

The vulnerability attribute that could be derived from Mapillary imagery was the wall material. The Mapillary platform enabled to automatically detect objects with computer vision technology. Objects such as buildings, pedestrians or even cars can be automatically identified from the street-level images. The method used by Mapillary is also based on image segmentation: each pixel in the image corresponds to a certain object class (Mapillary, 2019). Recently, the 510 team has developed a model for automated building material classification for Mapillary street view images, based on deep-learning. This model is used for the automatic classification of building material. The model enables to classify a building as either made of concrete, bricks or mud. The accuracy of the model is around 85%. The output of the model was a point map containing the recognised wall material label. The points represent the location from where the picture was taken, but do not identify to what building it belongs.

To allocate material points to the corresponding building, a new automated approach and a manual tool were developed by Mapillary after several expert discussions. This methodology was tested for the first time in this study. Summarised, this automated approach uses the unique photo ID of each point and sends it to the Mapillary API to request extra information about the image. In this case the the camera angle (in degrees) and the field of view (in radiance) were used. Those values were used to calculate the orientation of the picture on the map (either the left or right field of view from the point) and to calculate the exact point of direction, or angle, of the camera. Then, for each point, a line of 50 meters was drawn into the correct direction based on the field of view and camera angle. This line dataset could be added as a spatial layer. The intersection tool was used to merge the wall material attribute of each line with the OSM building that was the first to be crossed by the line.

The manual tool enables to click on the building in the OSM map that matches the building in the picture. By clicking on the building in the map, the wall material information is added in the corresponding attribute table. For each image separately, this process is repeated. In figure 10 a screenshot of the tool is presented. The tool is available here: https://mapillary.github.io/mapillary_solutions/building-labels/. In this research, a hundred buildings were manually enhanced with material information. These were used as 'ground truth' samples to measure the accuracy of the automated approach.

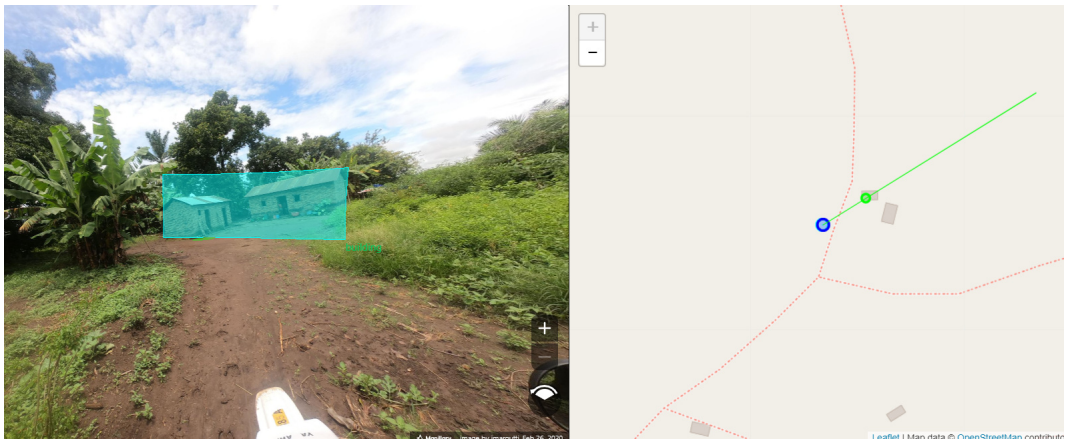

Figure 10: Mapillary tool for manual allocating buildings in OSM

UBR survey

The UBR survey contains indicators on social vulnerability, such as level of education, wealth, age, health and household size. Those indicators were used to create a composite vulnerability index for the 824 households that participated in the survey. The methodology was based on research by Adu et al. (2018) and the Handbook on Constructing Composite Indicators by the OECD (2008).

Because each indicator was measured on a different scale, the values were standardised as an index by using the min-max standardisation approach (OECD, 2008). The following equation was used to standardise the indicator values per household:

$$Index_{Shi} = \frac{Sh - s_{min}}{s_{max} - s_{min}} \tag{6}$$

Sh is the observed indicator sub-value for a single household. s_{min} and s_{max} are the minimum and maximum values in the range of the indicator.

In table 6 the minimum and maximum values of each indicator are listed. Those values were used as input for the standardisation equation. The column on the right lists the average index values for each indicator after the values were standardised.

Indicator	**Minimum value**	**Maximum value**	**Average index value**
Wealth	1 (poor)	3 (poorest)	0,344
Household size	1	13	0,792
Highest education	1 (none)	4 (training college)	0,327
Fit for work	0 (yes)	1 (no)	0,197
Age	1 (20-30 years)	7 (80-90 years)	0,420

Table 6: The minimum and maximum values of the indicators and the average index value

After the values were standardised, the following equation was used to create the SVI for each household.

$$SVI_h = \frac{\sum_{i=1}^{N} index_{shi}}{N} \tag{7}$$

Where SVI_h, the SVI index value of household h, equals the weighted average of the indicator values. The xy coordinates of the locations of each household were taken during the survey. The coordinates were plotted on the map to merge them with the corresponding OSM building.

4.3.2 Improving CAPRA vulnerability curves

As mentioned before, a common approach used to identify the vulnerability to flooding is by assessing the potential damage on the housing stock based on depth-damage curves. Depth-damage curves quantify flood vulnerability by relating water depth at the affected object to a damage grade (de Moel et al., 2015; Merz et al., 2014). It is important to use separate functions for different building material types, as, for example, a mud house will collapse at a lower water depth compared to a brick house. Due to the absent of reliable damage databases in Malawi, a synthetic damage curve approach will be applied in this research.

In the context of Malawi, Rudari et al. (2016) and Wouters et al. (2020) used damage curves derived from CAPRA (Comprehensive Approach to Probabilistic Risk Assessment), an open source software with the aim to improve the understanding of disaster risk for decision making and planning purposes. The software contains a physical vulnerability model which can be used for the development of physical vulnerability functions for specific hazards and asset classes (Reinoso et al., 2018). As depicted in figure 11, the curves exist for the building materials mud, concrete, wood and masonry. Rudari et al. (2016) aggregated the existing building stock materials in Malawi into the classes traditional, semi-permanent and permanent. Then, they linked the building materials to the most corresponding material in the CAPRA library.

This research uses a similar approach. Based on building typologies found in the Karonga district, the corresponding CAPRA material was linked. This process is depicted in table 7. The curves of the building materials were aggregated according to the three housing classes. Permanent buildings were classified as buildings with either concrete or brick walls and iron rooftops. Traditional buildings were classified as walls made of mud, reed or wood and roofs made of thatch. Semi-permanent buildings either have traditional walls and iron roofs or permanent walls and thatched roofs.

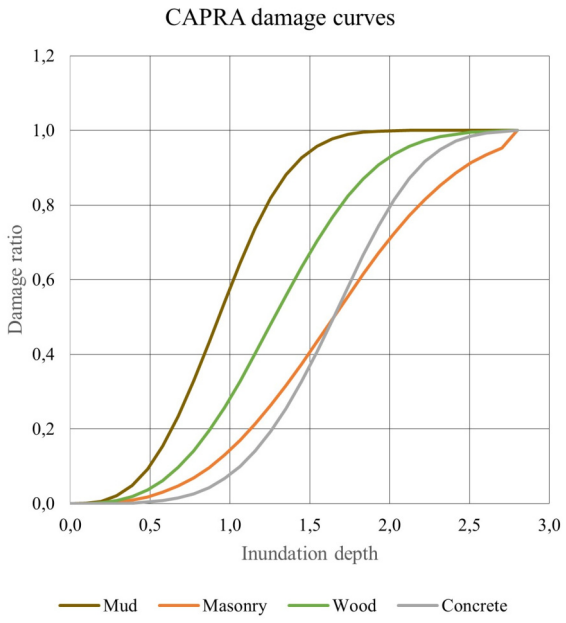

Figure 11: CAPRA curves for mud, masonry, wood and concrete

CAPRA material				Building stock materials	Housing typologies		
Concrete	Masonry	Earth	Wood		Traditional	Semi-permanent	Permanent
x				Concrete		x	x
		x		Mud/wattle	x	x	
		x		Reed/straw	x	x	
			x	Wood	x	x	
	x			Bricks		x	x

Table 7: The correspondence between housing typologies, building stock material and CAPRA material, adjusted from Rudari et al. (2016)

The curves were be manually adjusted according to damage data derived from the ECHO 3 survey. Based on several assumptions, an overview of the average damage per building type was created. The assumptions are described below:

In the survey, the water height of the flood was classified as ankle, knee, waist and shoulder length. It is assumed that:

- Ankle length means a water height of 30 centimetre
- Knee length means a water height of 50 centimetre
- Waist length means a water height of 1 meter
- Shoulder length means a water height of 1,5 meter

Flood damage was described according to the parts of the house that were affected during the flood. The damage classes in the survey were floor, walls, windows and roof. It is assumed that:

- A damaged floor means 20% damage
- Damaged floor and walls means 50% damage
- Damaged floor, walls and windows means 60% damage
- Damaged floor, walls, windows and roof means 80% damage

4.3.3 Fusing data layers

A spatial layer of the building extents in the research area was derived from OpenStreetMap. This layer is used as a base layer. The data layers containing vulnerability attributes were all merged with the overlapping OSM buildings to create a multi-attribute vulnerability layer. In cases where the layers with vulnerability attributes were not readily aligned with the OSM layer, several GIS techniques were be applied as listed in table 8. For example, the coordinates that were taken during the household survey were not directly linked to the building coordinates in OSM. In many cases this led to survey points located outside the house, making it difficult to rematch with the corresponding building. In this case, a spatial join has been applied in which a search radius of 10 meters around the building was added. The information of the nearest data point was then automatically added to the building. Moreover, to align the OSM data with the UAV imagery the 'move' tool was used.

Tool	Description	Implementation example
Move	Moves or rotates a feature or selection of features	Moving all features of a layer in a similar direction/angle simultaneously
Spatial join	Joins attributes from one feature to another based on a spatial relationship	Joining features within the distance of the search radius to match the closest point to a building
Align features	Identifies inconsistencies of the input features against the target features and aligns with the target feature	Aligning the polygon outline of one layer with another layer

Table 8: ArcGIS Pro tools for automatically aligning features

In total, 1400 buildings were delineated in the OSM base layer. However, the UAV, Mapillary and UBR datasets did not completely overlap with each other and with the OSM layer. Out of the 1400 OSM buildings, 831 buildings could be linked to the rooftop material attribute. Moreover, only a limited part of the Mapillary analysis was conducted in the research area, causing limited overlap with the rooftop layer. To increase the number of buildings with detected wall material, wall material data points derived from the ECHO 3 survey were added to the unidentified buildings. This resulted in the identification of both rooftop and wall material for 607 buildings. Lastly, 94 buildings could be linked to both the physical and social vulnerability attributes. All overlapping buildings are located in Traditional Authority Mwakaboko, which is part of the Karonga district. In figure 12 the amount of overlap between the datasets is depicted.

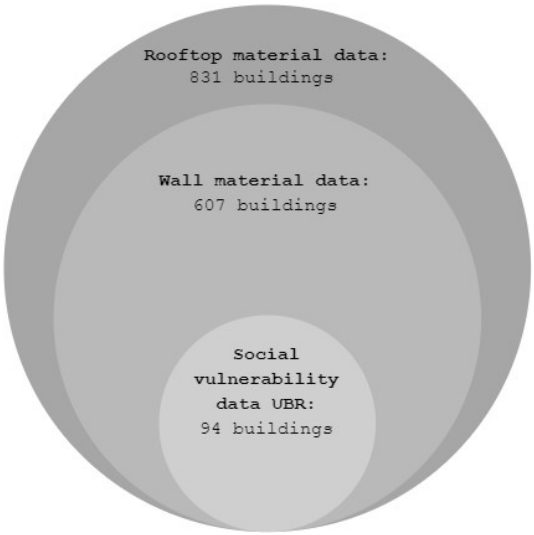

Figure 12: The overlap between the vulnerability attributes

4.3.4 Identifying patterns and clusters for up-scaling

This vulnerability assessment is based on small areas in the Karonga district in Malawi. This area has been thoroughly analysed by the Malawian Red Cross and therefore a wide range of data sources is available. However, it is preferable that the methods used in this research are applicable to a wider context as well. Therefore, this research attempted to explore the possibilities for up-scaling to areas where, most likely, less data sources are available. This was done in two ways:

1. By identifying the correlation between vulnerability attributes in the research area in a bivariate analysis

2. By creating a framework for the applicability of this assessment method at multiple scales

Bivariate analysis

To discover the relationships between the vulnerability attributes, a bivariate analysis was conducted. This type of statistical analysis aims to uncover whether or not two variables are related (Bryman, 2012). If the variables are related, the variation in one variable coincides with the variation in another variable (Bryman, 2012). The correlation statistic Pearson's r was used to discover the strength of the relationships. The correlation value lies between -1 and 1, where a value close to -1 indicates a negative relationship, a value close to 1 indicates a positive relationship. The closer the coefficient is to 0, the weaker the relationship. A coefficient can only be generalised if the level of significance is lower than 0,05 or 0,01.

It is important to note that the correlation coefficient only indicates the relationship between variables and not the causality. Meaning that it can not be inferred that one variable causes the other. However, strong correlations between the vulnerability attributes in this research can be used to do assumptions, although with high uncertainty, for areas in Malawi with a similar character. For example, if it seems that a certain type of rooftop material is in many cases related to the same wall material, it can be assumed that this relation exists in other Malawian rural villages as well. In that case, when UAV imagery is unavailable, satellite imagery can be used to identify rooftop material in those areas. Similarly, the survey data can be used to identify relationships between social and physical vulnerability. Based on these relationships, clusters can be created and predictions for other areas can be made. The aim was to use a geon-related approach for up-scaling to other areas by linking indicators that are known (e.g. rooftop material) to assumptions based on observed patterns in Karonga. However, as will be presented in section 5.3.4, only limited to no correlation could be identified between the attributes. This was the result of small overlap between the attributes, leading to a low sample size and a very unequal distribution over the classes. Therefore, sub-question 4 will be answered based on an analysis of the usability of the proposed methodology.

Framework for assessing usability at different scales

The first framework assesses the usability from a Disaster Risk Reduction perspective. Based on a literature review, several potential DRR interventions for the context of Malawi were classified according to their scale of impact. The scale concept was divided into the micro, meso and macro scale, based on Merz et al. (2010). For each DRR intervention, the required data and assessment methodology is listed. In order to outline the usability at different scales, the data types and assessment methodologies in the framework are comparable to the methods used in this research. The data types can either be based on UAV/satellite imagery or on survey data. The assessment methodologies are based on remote sensing, machine learning or surveying.

Moreover, the second framework discusses the applicability from a data availability perspective. For each scale, the required datasets are listed, together with the data level that can be used for aggregation. Moreover, examples for damage curves at different scales are presented.

5 Results

This section is built up according to the sub-questions of this research. First, it is described what vulnerability attributes were identified with the acquired datasets. Second, it is discussed how local damage data was used in adapting existing damage curves to the context of Karonga. The third sub-section describes how vulnerability assessment can be improved when combining datasets. The last section sheds light on the possibilities for up-scaling.

5.1 Characterizing housing stock attributes from UAV, Mapillary and household survey data

The findings in this section contribute to answering the first sub-question: *What physical and social vulnerability attributes can be derived from the acquired datasets?* Per dataset, the derived vulnerability attributes are presented and the outcomes are validated. The methodology has been applied on an area of around 6 square kilometer within the larger research area.

5.1.1 UAV data

The analysis with UAV imagery resulted in the identification of the rooftop material attribute. An OBIA was performed to classify the UAV imagery of the research area into multiple land use classes. The land use classes vegetation, shadow, bare soil and road were used to distinguish land from the rooftops. The rooftops were classified into either iron or thatch. No other rooftop materials could be identified in the research area. Iron has very unique spectral characteristics, making it easier for the machine learning model to distinguish from other land use classes. However, bare soil and thatch show similar characteristics, leading to confusion for the model when classifying both land use types. This is illustrated in figure 13. The upper-right image shows the classification of iron and thatch before filtering techniques were applied. Here, the iron rooftops are clearly recognisable as they are delineated realistically by the model. However, thatch is often incorrectly represented due to confusion with bare soil areas. This resulted in large areas misclassified as thatch, making it difficult to recognise thatched rooftops.

Several filtering techniques were used to erase ambiguously classified objects that did not represent buildings. First, a height threshold was added to filter out all objects with a height not corresponding building height. Second, a size threshold was added to erase objects that were either too small or too large to represent buildings. The bottom-left image in figure 13 illustrates the result. Here, it is visible that the thatched rooftops still have ambiguous shapes and in some cases do not represent a building. Therefore, an OpenStreetMap building layer of the research area was used as a base layer. The OBIA objects were joined with the overlapping OSM objects, resulting in clearly delineated buildings and the corresponding rooftop material. This is depicted on the bottom-right in figure 13.

Table 9 shows how the amount and size of the objects decreased after the thresholds were applied. It is clearly visible that the addition of thresholds had a significant effect on limiting the number of ambiguous objects. In table 10 the final amount of OSM objects for thatch and iron is depicted.

	No threshold		*Height threshold*		*Height + size threshold*	
Rooftop material	**Objects**	**Area (m2)**	**Objects**	**Area (m2)**	**Objects**	**Area (m2)**
Thatch	4182	376236	3488	76018	815	48417
Iron	2294	119672	1351	37568	546	32565
Total	6476	485908	4840	113586	1361	80982

Table 9: The number of objects and area size for buildings with thatched and iron rooftops, as classified in the OBIA. Calculated with different thresholds

Rooftop material	Percentage	Number	Area m2
Thatch	22,6	236	10435
Iron	66,0	594	36814
Undefined	7,8	70	2530

Table 10: The number number, size and share of OSM buildings classified as thatch or iron

Figure 13: Upper-left: the original UAV image; **upper-right**: the iron and thatch OBIA classification without thresholds; **bottom-left**: classification with height and size threshold; **bottom-right**: classification merged with OSM buildings

Validation

The results of the Object-Based Image Analysis were validated by comparing the classified segments with manually delineated samples. The model has an overall accuracy of 77,4% and a Kappa coefficient of 0,72, meaning that a substantial agreement between the classification and validation samples exists. The confusion matrix and corresponding statistics per land use class are summarised in appendix A. As previously mentioned, confusion between the classes 'bare soil' and 'thatch' resulted in 'thatch' being over-classified and 'bare soil' being under-classified. This is also visible when comparing the statistics of bare and thatch.

To measure the accuracy of the final classification where rooftop materials were merged with OSM buildings, the overall accuracy and Kappa coefficient were calculated. Ground truth samples

derived from the ECHO 3 survey were used to validate the predicted classified materials with real-life measurements. In total, 213 ground truth samples were used. With this, the overall accuracy of the model is 0,81, meaning that 81% of the predicted buildings reflect the real-life situation. However, when looking at the F-1 score of each individual class, iron performs better compared to thatch. The Kappa value is 0,51 meaning that a moderate agreement between the OBIA and ground truth data exists.

Material	Precision	Recall	F-1 score	Accuracy	Kappa
Thatch	0,67	0,49	0,57	0,81	0,51
Iron	0,85	0,92	0,88		

Table 11: Validation statistics for the OBIA classification

Moreover, The results of the model were compared with the results of the ECHO 3 survey (Appendix B). A similar distribution of buildings over the iron and thatch classes can be perceived when comparing the model output and survey results. Whereas the model classified 66% of the rooftops as iron, were 65% of the houses in the survey classified as iron. The model classified 22,6% of the rooftops as thatch and 7,8% as undefined. 32% of the buildings in the survey were classified as thatch.

5.1.2 Mapillary data

The Mapillary data was used to identify the wall material attribute. The output of the deep learning analysis was a point map of the picture location with the corresponding identified wall material. Although this gave an overview of the approximate locations of the building materials, it was not possible to directly link the material to the corresponding building. The picture angle of each point was calculated to gain understanding on the direction of the identified building. The angles were represented by lines and the corresponding building on the OSM map is the one that intersects the line first. This is depicted in figure 14.

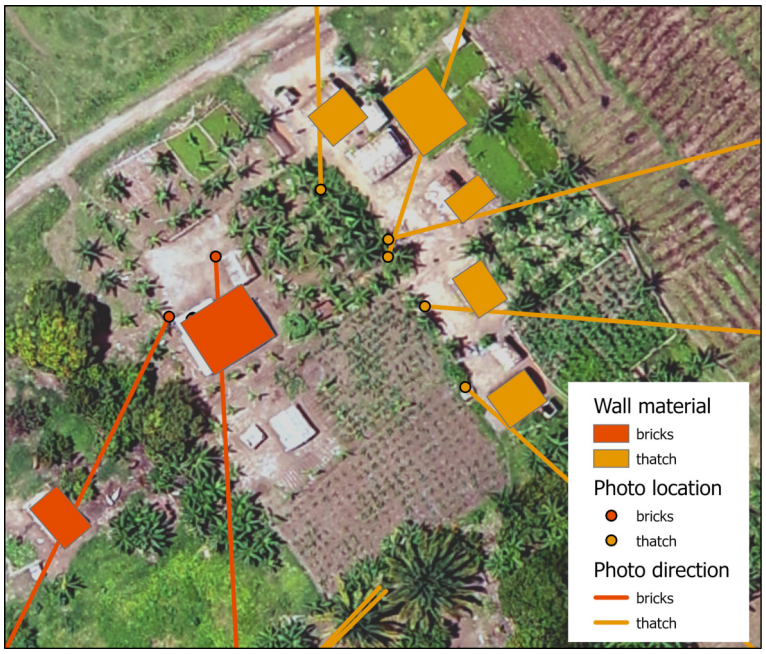

Figure 14: The process of matching the Mapillary photo point to the corresponding building, by making use of the camera direction

In total, the wall material of 294 buildings could be identified with the machine learning Mapillary analysis. The wall materials that could be identified in the research area were bricks, concrete and thatch. In table 12 the number of detected buildings per material class is given.

Rooftop material	Percentage	Number
Bricks	77	222
Concrete	15	43
Thatch	10	29

Table 12: The number of detected wall materials on OpenStreetMap buildings

Validation

The Mapillary model was tested on a random set of 889 images to assess the quality of the classification performance. The same accuracy statistics as for the OBIA assessment were computed for the classes 'bricks' and 'concrete'. There was insufficient information to compute the statistics for 'thatch'. The overall accuracy of the classification is 84%. When comparing the F-1 scores of the separate classes, it can be observed that 'bricks' performs relatively better than 'concrete'.

Material	Precision	Recall	F-1 score	Accuracy	Kappa
Bricks	0,99	0,66	0,80	0,84	0,68
Concrete	0,77	0,99	0,68		

Table 13: Validation statistics for the OBIA classification

To assess quality the automated join approach between data point and OSM building, a Mapillary tool was used that enables to manually link the building on a Mapillary image to the correct OSM builing on the map (see figure 10). In total, 118 buildings were manually linked with the tool to serve as validation samples. When comparing the automated output with the validation samples, 86% of the buildings were allocated correctly.

5.1.3 UBR survey

The UBR survey data was used to create a relative Social Vulnerability Index (SVI) based on the households in the research area. The indicators wealth, household size, education, health (fit for work), and age were used. The indicator values were all normalised into a range between 0 (low social vulnerability) and 1 (high social vulnerability). Moreover, the correlation between all the indicators was calculated, to observe the influence of each indicator. In table 14 it can be observed that the indicator 'fit for work' has the largest influence. Therefore a lower weight was given to this indicator during the calculation of the vulnerability index. Figure 15 illustrates the distribution of the resulting values over 5 classes. The average SVI score is 0,43, with the majority of households distributed over the classes that range from 0,21 to 0,6. This means that based on the indicators mentioned previously, those households live in situations of relative moderate social vulnerability. 215 households in the survey could be linked to buildings in the OSM layer of the research area. Due to privacy regulations, it is not allowed to show sensitive personal information that can be traced back to individuals. For this reason it was decided to not disclose this information on the household level.

	Wealth	H. size	Edu	FW	Age
Wealth	1	-0,219	-0,036	0,016	-0,041
H. size		1	-0,069	-0,130	-0,021
Edu			1	0,176	0,235
FW				1	0,755
Age					1

Table 14: The correlation (Pearson's r) between the index indicators. Light green: $p < 0,05$ Dark green: $p < 0,01$ N = 824

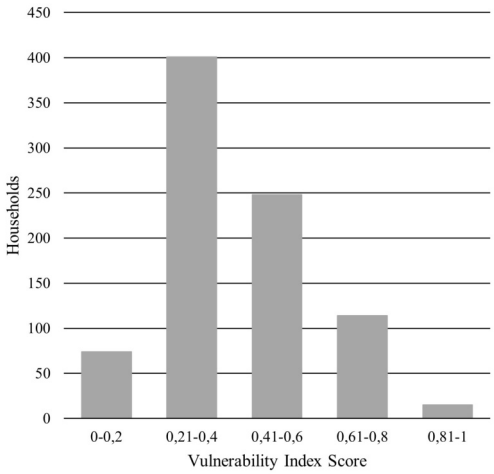

Figure 15: The distribution of households over SVI classes

5.2 Damage curves for Karonga

This section discusses the findings of the second research question: *How can local damage data be used to improve flood damage curves for Karonga?* Local damage data, derived from the ECHO 3 survey, was used to adapt the damage curves derived from CAPRA to the situation of Karonga. For each wall and rooftop material in the survey, the average damage was calculated for different flood levels.

Figure 16 shows that the CAPRA curve of mud has a damage ratio of 0,6 at almost one meter inundation depth. However, in the local damage data was found that at one meter inundation depth, damage was perceived on the floor, walls and roof. It is assumed that, when a building is damaged at the floor, walls, windows and roofs, a damage ratio of 0,8 can be expected. Therefore, a new curve was estimated that represents the average between the CAPRA and local damage data (see figure 16). This was also done for the masonry curve (see figure 17). Based on table 7 derived from Rudari et al. (2016) in the methodology section, the materials belonging to the traditional, semi-permanent and permanent building type have been aggregated to create the curves for each building type. In figure 18 the result is illustrated. In the next section, the curves are linked to the buildings in the research area to get an overview of the vulnerability at different flood levels.

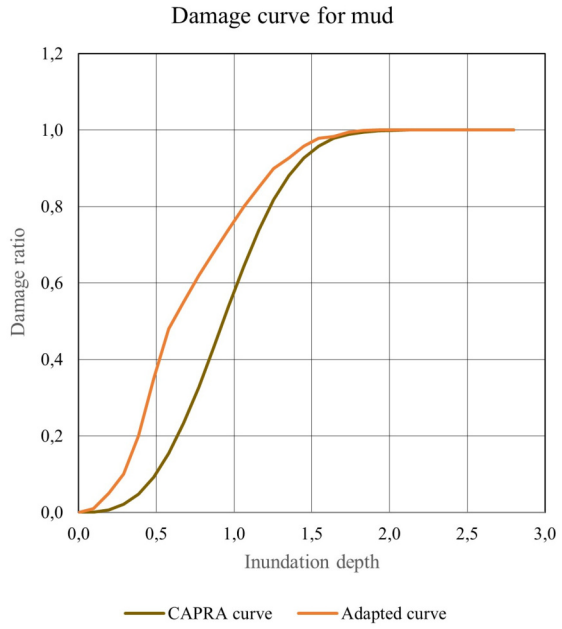

Figure 16: The CAPRA damage curve for mud and the curve adapted with local damage data

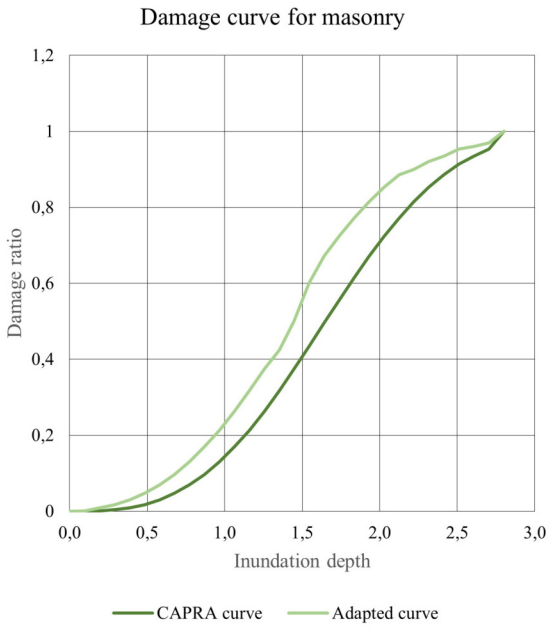

Figure 17: The CAPRA damage curve for masonry and the curve adapted with local damage data

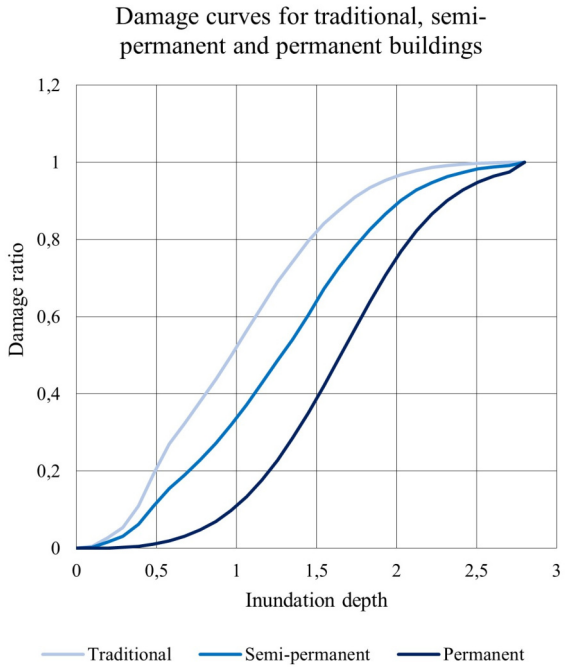

Figure 18: The damage curves for traditional, semi-permanent and permanent buildings, based on aggregated local damage curves

5.3 Vulnerability completeness

This section addresses the following sub-question: *SQ-4: To what extent do additional data sources add to the completeness of housing stock vulnerability attributes?* To explain the added value of combining datasets, several map visualisations are presented for several attribute combinations. Moreover, to identify relationships between the attributes, the correlation coefficients were calculated.

5.3.1 Combining physical vulnerability attributes

When combining rooftop and wall material data, the buildings can be classified according to the three building classes 'traditional', 'semi-permanent' and 'permanent'. All the buildings with thatched roofs and mud/thatched walls are classified as traditional. Buildings with iron roofs and brick/concrete walls are classified as permanent. All buildings with a combination of traditional and permanent materials are classified as semi-permanent. In figure 19, the spatial distribution of the buildings with the corresponding building type is mapped. This enables to identify physical vulnerability patterns throughout the research area.

In table 15, the proportion of buildings per type is summarised. The largest part of the buildings is classified as permanent, generally located in the western part of the area. Most of the permanent buildings tend to cluster along the M5 road, one of the largest roads in Malawi. The semi-permanent and traditional buildings are clustered along smaller roads in the eastern part of Mwakaboko. Moreover, the eastern buildings are located in a relatively lower-lying area compared to the buildings in the West. This makes them extra vulnerable during flood situations. The height difference between the western and eastern side is around 15 meters.

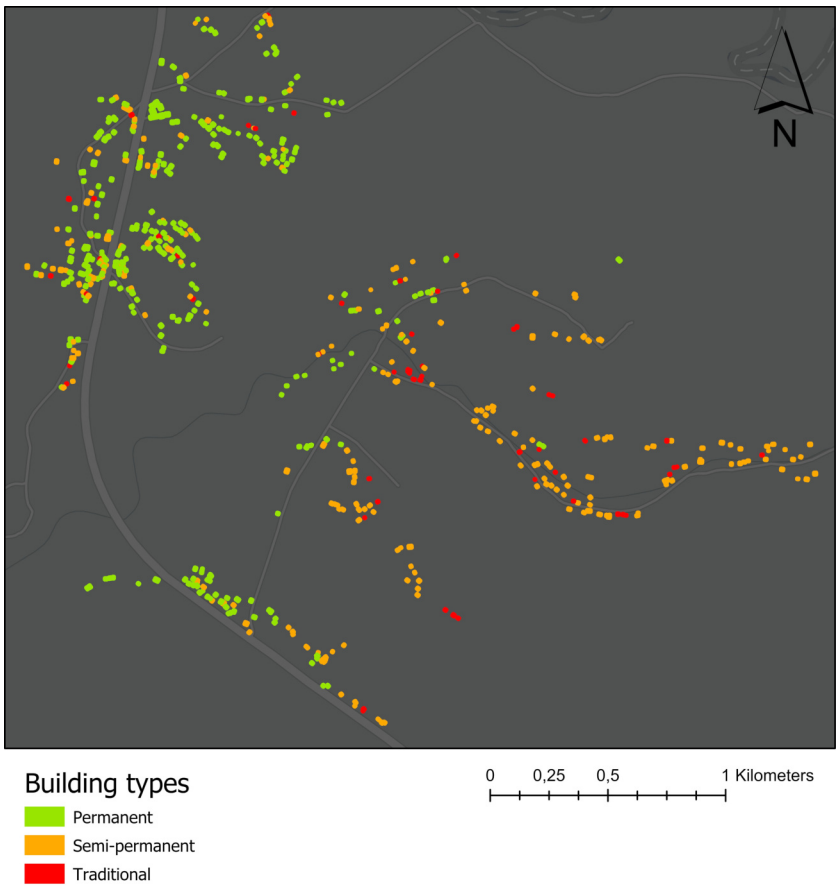

Figure 19: The spatial distribution of automatically classified building types in TA Mwakaboko, Karonga

The distribution of buildings over the three classes shows limited correspondence with find-

ings in the household survey (ECHO 3). In this research the majority of the buildings is classified as permanent (49,8%). In the survey, only 10% of the buildings was classified as permanent. Subsequently, the proportion of buildings classified as traditional or semi-permanent was significantly higher in the survey. However, the results show higher resemblance with the situation in the entire area of Karonga (table 1).

Building type	Percentage	Number
Traditional	9,2%	56
Semi-permanent	41%	249
Permanent	49,8%	302

Table 15: Distribution of automatically classified building types

5.3.2 Combining physical vulnerability attributes with damage curves

The building types correspond to the damage curves that were presented in the previous chapter. By linking the expected damage to the corresponding building types, synthetic 'what-if' analyses can be performed for different flood scenarios. In figure 20, the building vulnerability based on flood damage is mapped for three flood scenarios with: 1) an inundation depth of 0,5 meter, 2) an inundation depth of 1 meter, and 3) an inundation depth of 1,5 meter.

Whereas an inundation depth of 0,5 meter leads to 20% damage for traditional buildings, only 1% damage is expected for permanent buildings and 10% for semi-permanent buildings. Moreover, it is expected that at 1,5 meter inundation depth, traditional buildings are almost fully damaged. At the same inundation depth, it is expected that semi-permanent buildings are damaged for 60% and permanent buildings for 35%.

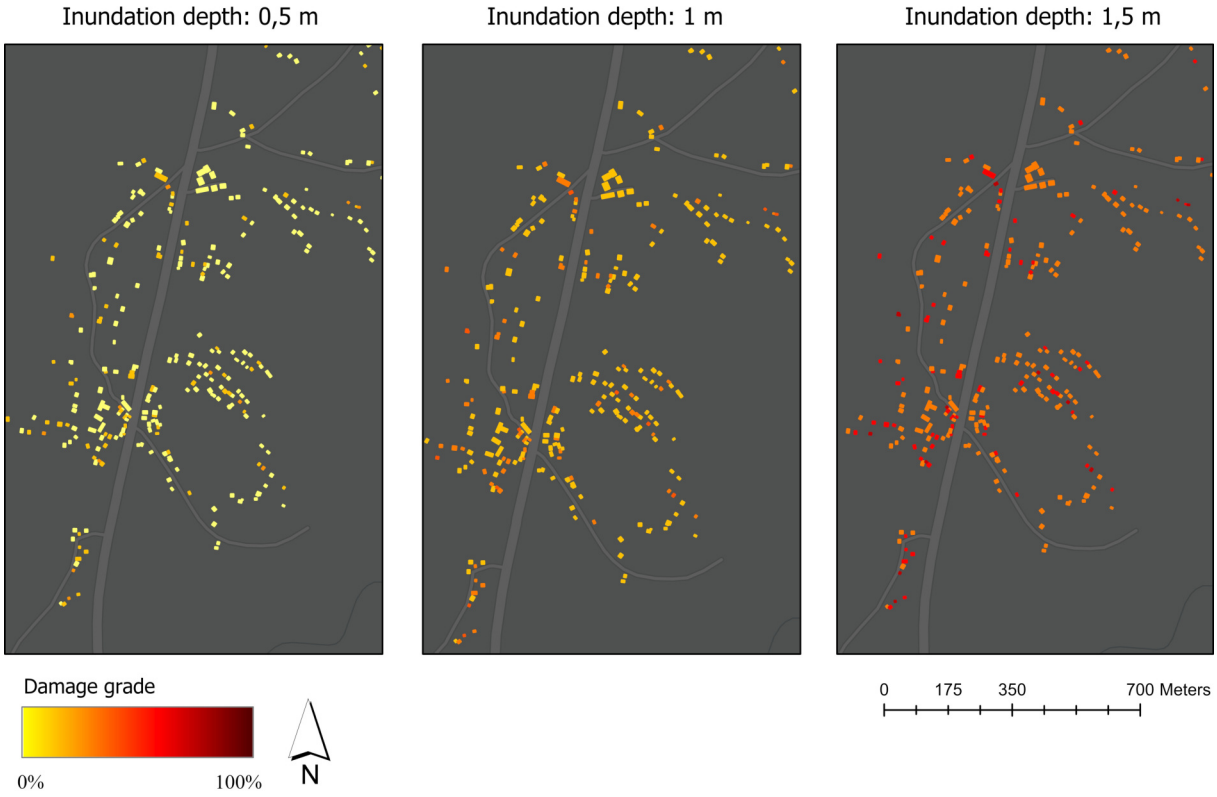

Figure 20: Building damage scenarios for different flood situations in Karonga, based on local damage curves

5.3.3 Combining physical and social vulnerability attributes

By linking social vulnerability to the physical attributes, an extra vulnerability dimension was be added. As previously mentioned in section 4.3.3, only limited overlap between the UBR survey and the physical vulnerability attributes exists. To increase the number of overlap, the wall material dataset was left out and the social index layer was joined with the rooftop material layer. In total, overlap between the two datasets for 175 buildings could be found. Based on these datasets, the average relative socio-physical vulnerability of the households is 0,34. This means that, compared to the social vulnerability index (figure 15) presented in section 5.1.4, the average vulnerability decreases when adding the attribute 'rooftop material' in the index. In figure 21, the spatial difference between the social vulnerability (right) and socio-physical vulnerability (left) can be observed. On the left map, the vulnerability decreased for a large part of the households. This means that, although the household is socially vulnerable, the building structure is relatively strong. However, for some households the vulnerability increased when the physical attribute was added. Meaning that those households are not only socially vulnerable, but also have limited protection due to poor housing.

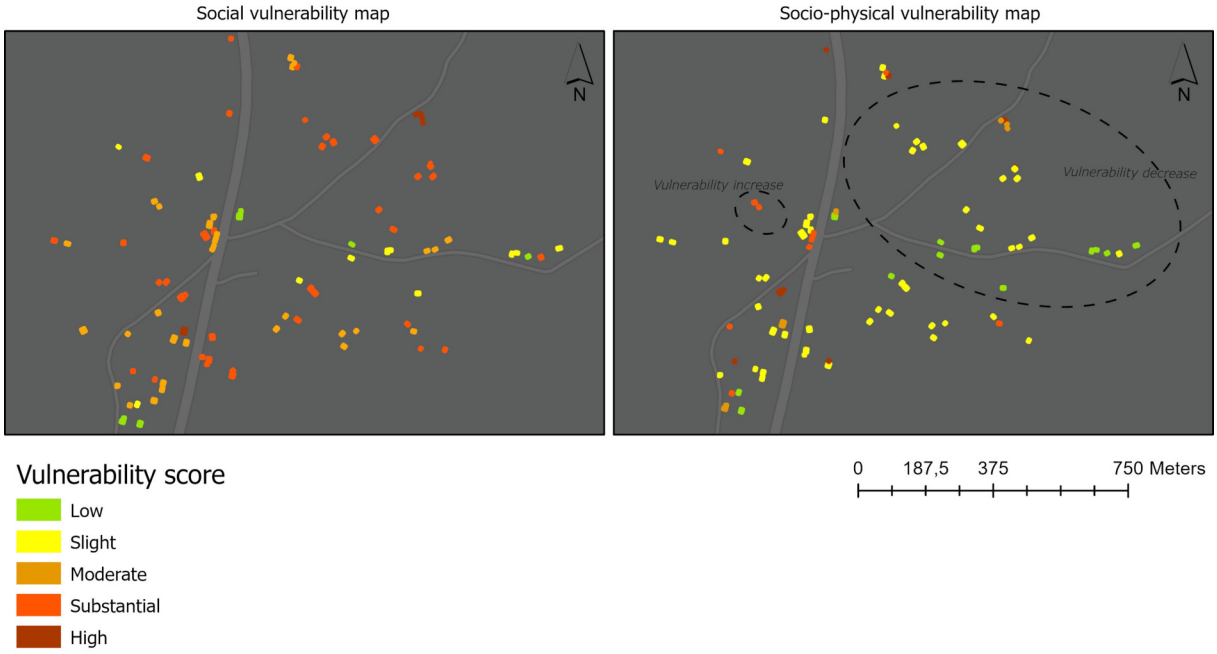

Figure 21: The difference between the social vulnerability and socio-physical vulnerability map

5.3.4 Correlation between attributes

By combining vulnerability attributes, the relationship between them can be analysed. First, the relationship between wall and rooftop strength has been observed. In the graph in figure 22 it can be observed that the majority of buildings with iron rooftops have walls made of bricks. Of the 308 buildings with iron rooftops, 85% has brick walls. However, for buildings with thatched rooftops, no clear relation with a specific wall material can be found. Pearson's r was calculated to identify the correlation between the attributes (see table 14). The correlation coefficient (r) between wall and rooftop strength is 0,191 with a significance (p) of 0,000, meaning that only a very limited positive and significant correlation between the attributes exists. Thus, a strong rooftop does not necessarily relates to a strong wall. However, the sample size (N) is relatively low due to limited overlap between the datasets and therefore it was not possible to calculate the correlation for the entire research area. This can influence the strength in correlation.

To see the effect of the sample size on the correlation level, the same calculation was done for wall and rooftop strength attributes derived from the ECHO 3 survey, with a sample size of 916

buildings. Here, a significant r of 0,697 was found, meaning that a medium to high positive correlation between the attributes exists.

Moreover, the relationship between physical and social vulnerability is observed. No correlation exists between building vulnerability (based on permanent, semi-permanent and traditional) and social vulnerability. Similarly, no correlation exists between rooftop vulnerability and social vulnerability. A medium positive, and significant, correlation between wall vulnerability and social vulnerability can be observed. In this case, this means that the higher the wall vulnerability, the higher the social vulnerability. This can also be observed in table 17, where the average SVI score increases when wall vulnerability increases. However, it is difficult to base conclusions on this data, as the amount of buildings in each class is not evenly distributed.

Relationships attributes	***r***	***p***	**N**
Rooftop vulnerability & wall vulnerability (ECHO 3 data)	0,697	0,000	916
Rooftop & wall vulnerability (classified data)	0,191	0,000	406
Building vulnerability & social vulnerability	0,064	0,538	94
Rooftop vulnerability & social vulnerability	-0,118	0,119	175
Wall vulnerability & social vulnerability	0,386	0,000	97

Table 16: The correlation (r) between physical and social vulnerability attributes, together with the level of significance (p) and sample size (N)

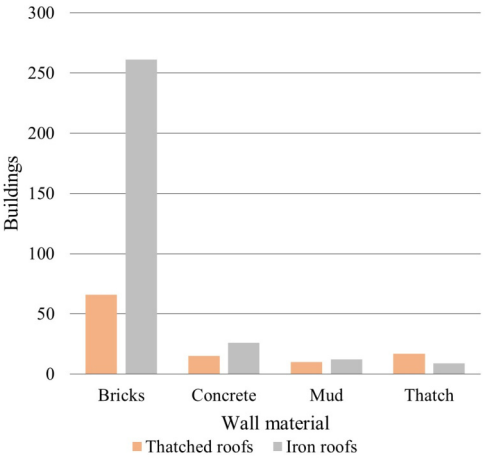

Figure 22: The distribution of buildings over rooftop and wall material classes

Physical vulnerability classes		**Average SVI score**	**Building count**
Building type	Traditional	0,75	3
	Semi-permanent	0,56	23
	Permanent	0,57	74
Wall material	Thatch/mud	0,87	8
	Concrete	0,61	6
	Bricks	0,54	86
Rooftop material	Thatch	0,53	49
	Iron	0,58	128

Table 17: The average SVI score and building count for each class of the physical vulnerability attributes

5.4 Scaling

The data availability and resolution in an area highly determine the possible scale of assessment that can be done. Subsequently, the scale of policy intervention largely depends on the level of the conducted risk assessment. As previously depicted in chapter 2, the complexity of data increases when the aggregation level decreases (Kienberger et al., 2013). The micro scale vulnerability assessment that is performed in this research has a low aggregation level, making the output data relatively detailed. However, this research was performed in an unique situation where a wide range of datasets was available. In other areas, it is very likely that the variability in datasets is not as high as in Karonga. For example, street view data is not available in every part of the world, and especially the most vulnerable areas are missing. In addition, high resolution UAV data only covers limited areas, necessitating the use of lower resolution satellite imagery.

The results that are presented in this section contribute to answering the last sub-question: *SQ 4: To what extent are the methodology and results of this micro scale study applicable to other scales?* In this section, the applicability of the methodology is discussed for the micro, meso and macro scale. The applicability is summarised in two different ways. First, in figure 24, the applicability is explained from a data availability perspective. In this figure the required datasets are presented for the three different scales, together with the possible level of aggregation that can be used. In the column on the right, flood damage curves are illustrated at the different scales.

Second, in table 18 the applicability is explained from a Disater Risk Reduction perspective. The table gives an overview of examples of DRR measures that can be taken at the micro, meso and macro level. For each measure, the data type and processing methodology required for the corresponding vulnerability assessment is given. Moreover, the table describes the level of data aggregation and complexity for the expected vulnerability data output. In the sections below, the implications for the application of this methodology are described for the different scales.

5.4.1 Micro scale

The vulnerability attributes that were derived during this research were based on UAV, Mapillary and survey data. An OSM layer of the building extents was used as a base layer. Local damage data was used to adapt the material-based damage curves derived from CAPRA. This resulted in the acquisition of a wide range of attributes to assess the vulnerability at the micro level, involving the buildings in the area.

In figure 8, an overview of the methodology is given. This methodology can be adapted to the data availability in the area to be assessed and data processing steps can be left out if the data availability in the area is lower. If, for example, only UAV data is available, it is still possible to derive vulnerability attributes that enable to give a substantial overview of the physical vulnerability. Although rooftop information is not the most important vulnerability attribute when assessing flood risk, it can be of great importance in the context of other natural hazards, such as earthquakes and heavy rains. In such contexts, the Mapillary analysis can be considered to be eliminated from the workflow.

Moreover, besides the indicators and processing steps, figure 8 lists the usability of each output dataset. The methodology can be adapted according to the required usage of the output data. In table 18 several examples of micro-scale DRR interventions are given, such as building strengthening prior a flood or resource distribution after a flood. An important response to realise these measures is to locate the most vulnerable households in an area. This requires object-level data on the physical state of the building or on the social vulnerability of the household. As mentioned before, the level of aggregation in micro-scale assessments is low, resulting in a complex, or highly detailed, data output. This type of assessment is useful for humanitarian agencies to efficiently indicate where the highest impact of a flood can be expected and where the help is mostly needed.

5.4.2 Meso scale

The meso scale represents spatial aggregations such as villages or river basins (Merz et al., 2010). Whereas micro-scale assessments aim to observe the spatial variability of vulnerability within, for example, a village, do meso-scale assessments observe the variability between different villages. This can be used to target and prioritise the most vulnerable areas when distributing resources or when stipulating locations for awareness campaigns. The meso scale interventions as presented in the table aim to structurally decrease flood vulnerability in the longer term. The interventions can either be implemented by governmental agencies, or during long-term humanitarian projects.

Two different approaches can be used for meso-scale assessment. First, when available, micro-scale vulnerability data can be aggregated to the meso level. This means that the average vulnerability of households is calculated for a certain area. Second, as UAV imagery is generally not available for an entire area, satellite data can be used as input data for OBIA. For the identification of social vulnerability at the meso scale, focus groups can be held as an alternative to household surveys. Focus groups enable to get an overview of the overall vulnerabilities and needs within a village (VCA, 2020). The damage curves in meso-scale assessment can either be based on aggregated material based curves (e.g. by clustering materials into building classes), or on broader land use classes such as urban, rural.

When aggregating data to the meso-scale, several levels can be considered. Officially, Malawi can be divided into districts, Traditional Authorities or Group Village Headman areas (GVH's), ranging from large to small respectively. However, assessments at the meso-scale are generally conducted in areas smaller areas, making official administrative boundaries unsuitable as aggregation level. In Malawi, official lower scale sub-divisions (e.g. village level) of the country do not exist. Therefore, the use of informal boundaries can be a good alternative in this case. For example, the GRID3 Malawi Settlement layer divides the country into areas based on their building density, i.e. built up areas, small settlement areas and hamlet areas, ranging from areas with high to low building density (CIESIN, 2020). Moreover, equal sized hexagons or circles can be used to form clusters if regions based on formal boundaries are too large. This is depicted in figure 23. Each hexagon represents the average vulnerability situation in that region. This approach enables to go beyond true boundaries during the scaling process and allows for the identification of vulnerability 'cold-' and 'hot-' spots of in the larger region.

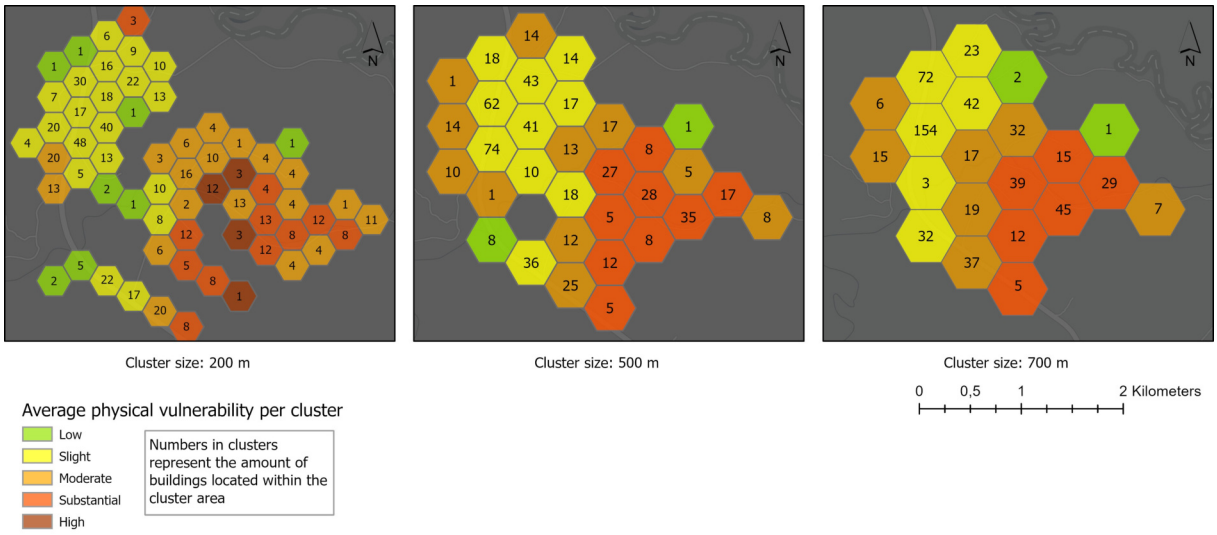

Figure 23: Example of aggregating local scale data: clusters representing the average physical vulnerability of the buildings located within the cluster

5.4.3 Macro scale

The macro scale covers the district, regional or national level (Merz et al., 2010). At the national level, large scale restructuring programmes can help in promoting flood-resilient building structures to decrease vulnerability. An example is the "*build back better*" strategy that was implemented by the Malawian government after severe floods in 2019. The strategy includes promoting resilience by adopting hazard-resistant construction standards and by improving the physical planning system (Malawi Government, 2019). For the prioritisation of the most vulnerable areas within the country, a high data aggregation level (e.g. district or TA level) can be used. To assess the vulnerability at this scale, satellite data can be used to distinguish between land use types. Moreover, elevation data can help in identifying areas located at river runoffs.

Macro scale assessments can be based on aggregated micro/meso-scale data or on satellite-based remote sensing. A common practice for the development of national flood maps is to merge existing micro and meso scale datasets into one map. However, difficulties can arise when making comparisons between areas where different assessment techniques have been used (de Moel et al., 2015; Loos et al., 2020). It is therefore important to carefully take into consideration the methodology and accuracy of each assessment. In figure 24, an example of a land use-based damage curve is given. This type of curve gives insight in the vulnerability of specific land use classes. For example, bare soil is more vulnerable to a flood compared to vegetated soil. It can therefore be expected that buildings placed on bare soil are more susceptible to flood damage compared to buildings surrounded by vegetated soil. Land use-based damage curves can therefore help in giving insight in the vulnerability of the country based on coarser land use classes.

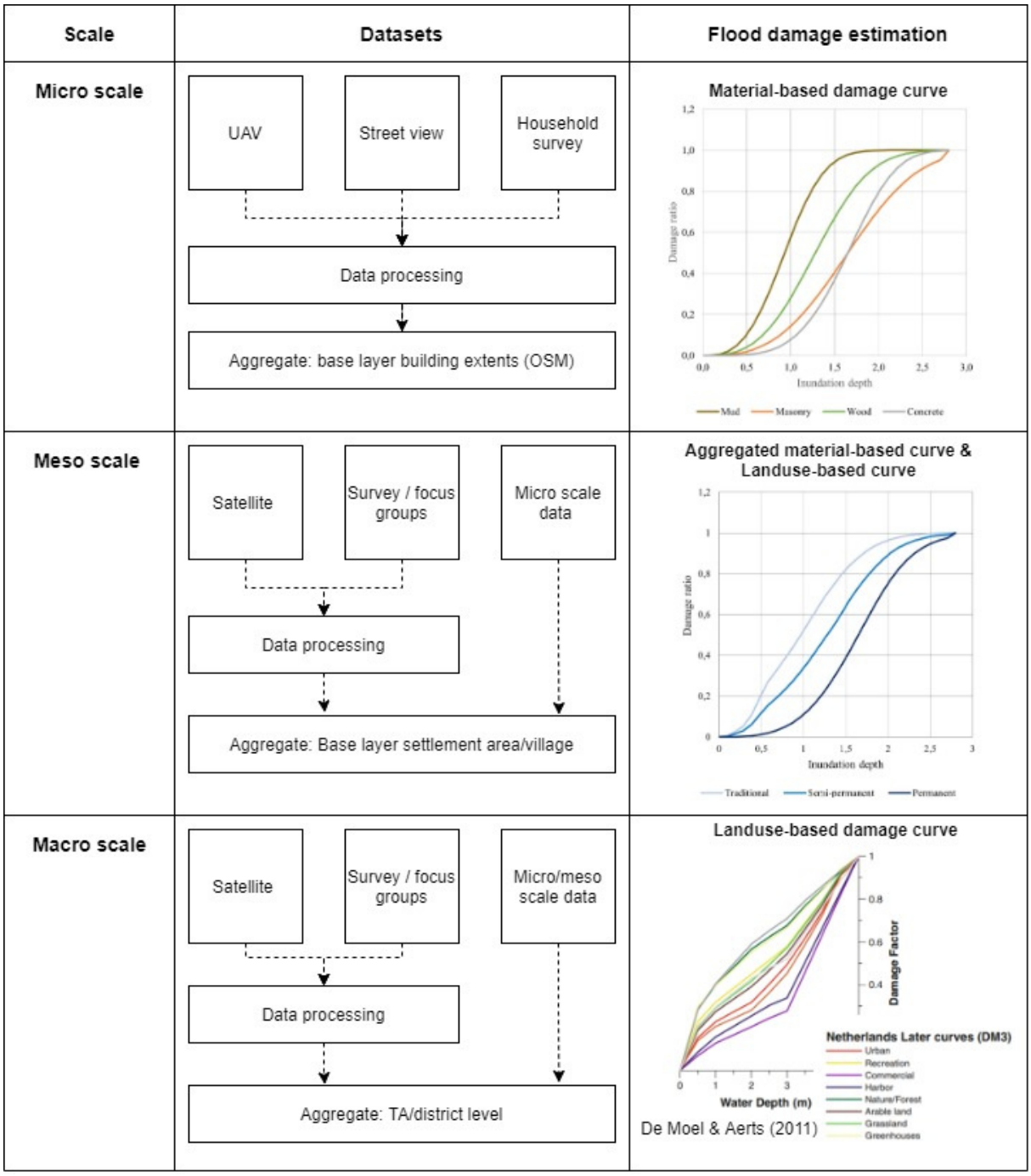

Figure 24: Summary of the required datasets, aggregation levels and flood damage curves for different scales of vulnerability assessment

Scale	DRR intervention	Response	Required data type	Method	Level of aggregation	Complexity
Micro	Strengthening wall/ rooftop material (VCA, 2020; Shelter, 2015)	Locating and prioritising the most physically vulnerable buildings	- UAV imagery - Satellite imagery - Street view data	- Survey - Remote sensing - Machine learning	Low	High
	Increasing building height (Shelter, 2015)					
	Protecting buildings by increasing green density (Shelter, 2015)	Identifying areas of bare soil surrounding buildings	- UAV imagery - Satellite imagery - Vegetation data	- Remote sensing	Medium	Medium
	Resource distribution	Locating and prioritising the most vulnerable households (physically and socially)	- Combination of social and physical vulnerability data	- Survey - Remote sensing - Machine learning	Low	High
Meso	Flood risk awareness education campaigns (VCA, 2020)	Targeting the schools in the most vulnerable areas	- Aggregated vulnerability data	- Focus group - Survey - Clustering of local data	Medium	Medium
	Flood-resilient building construction education (VCA, 2020)	Targeting areas with high numbers of traditional buildings	- Aggregated physical vulnerability data	- Clustering local data	Medium	Medium
	Promoting resilient land use practices (Shelter, 2015)	Targeting agricultural areas prone to floods/erosion	- Satellite / land use data	- Remote sensing	Medium	Medium/ high
	Resource distribution	Prioritising the most vulnerable settlement areas	- Aggregated social/ physical vulnerability data	- Clustering - Hot spot analysis	Medium	Medium
Macro	Land use planning (e.g. Built Back Better initiative) (Malawi Government, 2019; Shelter, 2015)	Targeting the most vulnerable districts/TA's	- District level/TA data - Satellite data - Census data	- Large scale survey - Remote sensing	High	Low

Table 18: DRR interventions and response at the micro, meso and macro scale, together with the required data and assessment methodology

6 Discussion

The objective of this research was to improve the understanding of the physical and social flood vulnerability of households in the Karonga district by combining multiple data sources. A remote approach was used to identify physical vulnerability indicators. UAV data was combined with street-level Mapillary data to get an overview of both the rooftop and wall materials of the buildings. For the identification of the social vulnerability, a Social Vulnerability Index was created based on indicators derived from survey data. This research developed an approach for the integration of all data sources into one Geographic Information System, based on an OpenStreetMap building layer. Local damage data was used to improve material-based damage curves and multiple "what-if" analyses were performed to get insight in the potential building damage at different flood stages. By combining the data sources, the level of detail in vulnerability assessment is greatly enhanced.

In this chapter, the methodology and results will be discussed. Firstly, some of the improvements in vulnerability assessment are discussed. Secondly, the usability for local scale interventions is outlined and examples of DRR interventions are given. Lastly, the validity and limitations of this research are discussed.

6.1 Implementation of the methodology

The chosen methodology enables to remotely characterise physical vulnerability attributes from UAV and Mapillary data. Moreover, it integrates social vulnerability attributes to increase the detail in vulnerability assessment. The remote characteristic of the methodology is suitable in areas where cadastral datasets are unavailable or nonexistent. This method is especially useful in times when physical visitation to a country is impossible due to, for example, conflict, pandemic, etc. Moreover, it is a promising time-saving alternative compared to carrying out household surveys. The methodology can be adapted to the data availability or the required intervention in other target areas. Several improvements for vulnerability assessments are discussed below.

Increased variability and accuracy

The methodology allows for the characterisation of housing stock vulnerability at the micro or object level. Contrary to vulnerability assessments based on aggregated land use data, object-based data shows the variability of vulnerability within a larger area. The classification methodology by Wouters et al. (2020) was broadened by incorporating the observed wall material and by adding the social vulnerability concept. Wouters et al. (2020) based their building classification on a combination of remotely sensed rooftop characteristics with vulnerability assumptions derived from a sample size of 50 buildings. Based on this combination, two different vulnerability types were developed. In this research, the vulnerability classification is enlarged by incorporating extra classes based on wall material and social vulnerability. Instead of using assumptions, this research uses the actual observed wall material. This significantly increases the accuracy of the physical vulnerability layer and allows for higher accuracy in damage predictions.

Linking UAV and street-level data

This research links UAV and street-level data to optimise the automated recognition of physical vulnerability indicators. For the purpose of this research, a tool was developed by Mapillary to automatically link information in a Mapillary image to the corresponding building in OSM. By making use of the camera angle, it is possible to allocate recognised objects in street view imagery to their original location on the map. By applying this methodology, object features can be identified from different perspectives. In this research, this resulted in the automatic identification of both the wall and rooftop material of a building. This resolves prior problems that generally come assessments purely based on nadir-view imagery, as mentioned by Wouters et al. (2020) and Cao et al. (2018).

Integration in early warning systems

As mentioned before, humanitarian actors are increasingly shifting their focus away from post-disaster recovery to preparedness and early support before a disaster occurs (De Perez et al., 2016). The concept of Forecast-based early action (FbA) is one of the mechanisms that is used to translate hazard warning information into concrete action (Wilkinson et al., 2018). FbA is used to trigger humanitarian intervention for the most vulnerable households in the hazard area (De Perez, 2018). To assess the impact of a hazard on the society, an integration of hazard forecasts and vulnerability data is essential.

The integration of vulnerability data with a high level of detail can be imperative in assessing the hazard impact. FbA mechanisms generally make use of pre-established thresholds or 'danger levels'. If a threshold is met, funds are released or action can be initiated (Wilkinson et al., 2018). Based on damage curves that were created in this research, local vulnerability or damage thresholds per building type can be enabled. If, for example, a damage threshold of 50% is incorporated in an early warning system, a warning can be given when a flood is expected to exceed the threshold level. For traditional buildings, the threshold level of 50% is reached at 1 meter inundation depth. For semi-permanent buildings, the threshold is reached at 1,2 meter inundation depth. In combination with the physical vulnerability layer, this situation is mapped in figure 25. The black buildings represent the buildings that would exceed the damage threshold at an inundation depth of 1,2 meter. Comparable maps can be used for the prioritisation of the most vulnerable households in getting support prior to or after a flood.

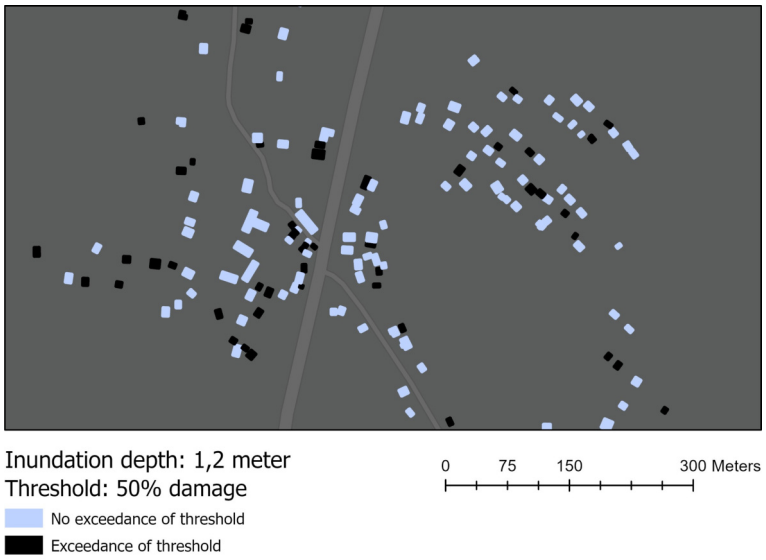

Figure 25: An example of a visualisation of flood vulnerability based on a 50% damage threshold

6.2 Usability for local scale interventions

Flood related interventions can be aimed at different components of risk. Structural measures are used for improving disaster prevention, whereas non-structural measures involve awareness-building and improving planning and response capacity (Wisner et al., 2018). In March 2020, a Vulnerability Capacity Assessment (VCA) was performed in Karonga. The assessment revealed that the largest flood vulnerabilities of the society are the loss of houses and the lack of response skills and tools (VCA, 2020). To combat such vulnerabilities, several Disaster Risk Reduction strategies can be taken. The social and physical vulnerability map created in this study, give a detailed overview of the spatial distribution of the vulnerabilities in the area. The map can therefore serve as a base for initiating local DRR strategies in the area.

The different building typologies in the area ask for different strengthening approaches. De Ruiter et al. (2020), for example, mention potential measures per building type that can be

applied during building strengthening projects in a flood-prone area in Afghanistan. They argue that buildings made of wood or mud have a tendency to either flow due to lightweightness or collapse during intensive contact with water. For such buildings, a mixture with adobe or concrete would help in increasing the resistance of the walls. Moreover, stilts can be used to increase the height of the buildings to decrease the susceptibility when a flood hits the area. Moreover, Shelter cluster (2015) published a document with detailed building safety measures for Malawi that can be implemented to decrease the impact of floods. A detailed description for strengthening the building construction of informal buildings, in the context of Malawi, was published by Bureau TNM (2016).

The physical vulnerability map can be used to target the households that are the most physically vulnerable. Moreover, cost estimations can be made when the amount of target buildings and the corresponding measures are calculated.

The lack of response skills and tools in the communities cause increased vulnerability when a flood hits the area (VCA, 2020). By integrating flood awareness in school programmes or by organising awareness campaigns for adults, the communities are strengthened in their capacity to respond to hazards. In addition, increased awareness helps encourage communities to identify vulnerabilities in their settlements and in establishing local contingency plans.

Here, the social vulnerability map serves as a tool for identifying the most vulnerable communities in the area. Consequently the schools in vulnerable areas can be targeted as locations for awareness campaigns. Moreover, the most physically vulnerable areas can be identified for carrying out training concerning resilient building practices.

6.3 Validity and limitations

This research is performed in TA Mwakaboko in the Karonga district. Due to limited overlap between the datasets, it was not possible to assess the vulnerability of the entire housing stock. 607 out of 1400 buildings could be automatically classified. Only 90 of those buildings could be linked to the social vulnerability attributes. Due to this minor overlap, it is difficult to detect a possible relationship between the variables/attributes that can be generalised to other areas in Malawi. Therefore, assumptions based on this research should be taken with caution

Although a strong relation has been found between iron rooftops and brick walls, the relation between thatched roofs and wall materials seems less strong. Moreover, no clear relation between physical vulnerability and social vulnerability can be observed. However, when incorporating other spatial variables, such as distance to main road or elevation, it can be observed that physically strong buildings are generally located at more favourable places compared to weaker buildings.

Difficulties arose during the classification process of thatched roofs. The problems related to this process are twofold. First, similarities in spectral characteristics between bare soil and thatch led to confusion during the machine learning classification. This resulted in large areas of bare soil being classified as thatch. Similar difficulties were perceived by Wouters et al. (2020). It is therefore unavoidable to incorporate an extra processing step by filtering on polygon height and size. Second, the building extents of OSM were used to filter the buildings from the OBIA and to eliminate ambiguously classified objects. Although the OSM layer was updated recently during a mapathon, not all buildings were delineated. Especially thatched buildings were underrepresented in the layer. This can be explained by the coarser resolution of the satellite data, making it more difficult to identify thatched rooftop with the unaided eye. The buildings that were not delineated in OSM were excluded from the research, resulting in a lower number of, especially thatched, buildings compared to reality. It is therefore crucial to stipulate that, based on the rooftop material, the physical vulnerability in the research area is higher than presented in this research.

As mentioned before, damage curves cause a lot of uncertainty due to their simplistic representation of a complex process. Reliable damage data on traditional building materials is scarcely available, which makes it difficult to apply curves to other contexts (Kellermann et al., 2020). In this research, local flood damage data, derived from the ECHO 3 survey, was used to adapt the curves to the context of Karonga. However, the building damage in the survey was expressed according to subjective damage classes, based on the damaged elements (e.g. floor, wall, windows). An inventory of the corresponding damage grades was missing and therefore several assumptions had to be made to translate the data to a curve. Moreover, it is important to note that the damage maps, resulting from the 'what-if' analyses, do not represent the actual building damage that was observed after a flood. The maps give an example of the vulnerability situation at different flood scenarios and can serve as a tool to base DRR measures on. Merz et al. (2007) discuss the problem of fictitious accuracy, which can occur when interpreting object-level vulnerability maps. The great detail that can be reached in such maps, distracts from the uncertainty that comes with synthetic damage assessments. Consequently, it is important to raise the users' awareness of the limitations and the purpose of maps (Merz et al., 2007).

Merz et al. (2007) mention that flood maps have to be updated continuously to take into account developments that have affected the flood or vulnerability situation. Moreover, they argue that the rate of change in flood hazard can be expected to be small, but the rate of change for vulnerability can be way more dynamic as a result of e.g. variability in flood risk awareness or changes in assets of the community. It is therefore important to note that the vulnerability maps, as presented in this research, represent the physical vulnerability situation of March 2020 and the social vulnerability situation of April 2018. A new flood can have a large impact on the area, increasing the uncertainty of the current maps. It is therefore important to repeat this assessment over time.

7 Conclusion and recommendations

7.1 Answering sub-questions

The sub-questions as proposed in chapter 3 have been answered throughout this research. The answers to these question are summarised in this section.

***SQ 1**: What social and physical vulnerability attributes can be derived from the acquired datasets?*

In this research, a range of vulnerability attributes were derived from a combination of datasets, as collected by Malawi Red Cross. For the identification of the rooftop material attribute, an Object-Based Image Analysis was performed on UAV imagery, resulting in a classification between thatch and iron rooftops with an overall accuracy of 81%. The methodology is suitable in areas where spectral characteristics of rooftops significantly differ from the characteristics of the subsurface. Challenges arose when distinguishing thatched rooftops from bare soil due to similarities in colour. Subsequently, this lowered the quality of the classification for this class.

The automated Mapillary classification resulted in the recognition of wall materials. A model for the automated classification of wall materials, developed by 510, was applied for this process. To allocate the resulting data points to the correct building, camera angle data was computed to identify the direction of the Mapillary images. With this approach, 86% of the data points were allocated to the correct building. It can therefore be concluded that this method is promising for mapping objects that were recognised from street view imagery.

By weighting the social indicators (wealth, household size, education, health and age) derived from survey data, a Social Vulnerability Index was developed. On a scale from 0 (low vulnerability) to 1 (high vulnerability), a relative average social vulnerability score of 0,43 could be observed in the area.

***SQ 2**: How can local damage data of Karonga improve existing flood damage curves?*

In this research, local damage data was acquired by aggregating the average building damage per flood depth. Several assumptions were made to transform the data to damage grades. Existing damage curves, derived from the CAPRA library, were tuned to the local findings. The approach of Rudari et al. (2016) was used to aggregate the curves into the three building classes (traditional, semi-permanent and permanent), to link them to the classified building map. It can be concluded that material-based synthetic damage curves are a good starting point when assessing physical vulnerability, but that it is of great importance to enrich them with local damage data. In this research the local damage data showed severe damage results compared to the CAPRA curves. For example, where the CAPRA curve for mud presented a damage ratio of 0,6 at an inundation level of 1 meter, did the local curve show a damage ratio of almost 0,8.

***SQ 3**: To what extent do additional data sources add to the completeness of housing stock vulnerability attributes?*

Combined, the UAV and Mapillary analyses allowed for detailed insights in the structural permanence of the buildings. Moreover, this enabled this research to observe the spatial pattern of physical vulnerability in the research area. By combining physical vulnerability data with damage curves, the average damage ratio for each building was estimated for multiple flood scenarios.

For the buildings where overlap was found between the social and physical vulnerability data, a relative Socio-Physical Vulnerability Index was developed. The average of this index was 0,34, meaning that the relative vulnerability slightly decreased when physical attributes were added to the index. Moreover, this allowed for the identification of relationships between the socio- and physical vulnerability of the households. However, due to limited overlap, the sample size of the buildings was relatively small. The distribution of buildings over the vulnerability classes was very uneven, resulting in insignificant correlations.

The multi-attribute dataset gave a detailed overview of the housing stock vulnerability in the research area. However, the small overlap between the buildings decreased the ability to generalise findings based on the building sample. A larger overlap is essential in increasing the completeness of the data.

***SQ 4**: To what extent are the methodology and results of this micro scale study applicable to other scales?*

The applicability of this method on other scales is highly dependent on the data availability in the target area. The data resolution can impact the assessment output and largely determines the detail that can be reached. This also influences the accuracy of the response for the DRR intervention.

This methodology can be adapted to other micro-scale contexts by eliminating indicators and corresponding processing steps based on data availability in the area. UAV imagery can be replaced by satellite imagery to increase the data coverage on the larger scale. Moreover, land use-based damage curves can be used if object-based data is unavailable. It is important to clearly establish the goal of the assessment to determine the suitable level of data aggregation. This can help in overcoming a mismatch between the data complexity and the intended response.

The current correlation results do not allow for up-scaling to other areas. More research is required to establish grounded assumptions with less uncertainty.

7.2 Answering main research question

In what way can UAV, Mapillary and household survey data be combined in order to assess housing stock vulnerability to floods in Karonga, Malawi?

This research aimed to build a bridge between individual datasets. Moreover, it attempted to cover the vulnerability concept as thorough as possible by linking both physical and social vulnerability attributes into one Geographic Information System. A remote approach was used to identify physical vulnerability attributes. Based on Mapillary API information, wall information could be linked to remotely sensed rooftop information of the same building. Compared to previous research, this method allows for higher accuracy in the classification of physical building characteristics. Moreover, when combined with social vulnerability attributes, an even higher level of detail can be achieved. The integration with depth-damage curves resulted in the recognition of flood impact on the housing stock. The uncertainty that is associated with damage curves can be decreased by attuning these curves with local damage data.

These advancements in object-based vulnerability assessment can be applied to improve targeting of the most vulnerable households in disaster response situations. This facilitates both governmental and humanitarian organisations in effectively achieving risk reduction in flood-prone communities.

The aim of this research was to discover statistical relationships between variables to be used for vulnerability predictions in other areas. However, it is essential when establishing a statistical justification that there is a significant overlap between different data sets. This was not the case in this research and therefore the observed relationships were unsuitable for up-scaling. Despite this, the methodology forms a basis for up-scaling to other contexts or scales. Based on data availability and the required DRR intervention, the methodology can be adapted to become applicable to the right context.

7.3 Recommendations for future research

7.3.1 Scientific community

To improve the recognition of thatched rooftops, future research should focus on other land use classification methodologies. This can either be done by comparing the performance of several supervised learning algorithms, or by comparing the results with classifications based on Convolutional Neural Networks and deep learning.

To increase the number of physical vulnerability attributes, future research can be focused on the recognition of other building features in Mapillary. The current 510 model allows for the identification of wall material. However, attributes such as openings in the building or the state of the buildings could be useful indicators as well.

Lastly, the relationships between vulnerability variables should be further investigated to be able to make statistically sound assumptions for other areas in Malawi.

7.3.2 Humanitarian agencies

The approach used in this thesis showed that combinations of datasets can increase the detail in vulnerability information. The datasets used in this research, were already collected before the commence of this research. Therefore, no influence on the data collection process could have been exerted. This resulted in limited overlap between the datasets and a lower amount of buildings that could be incorporated in the research. This approach can be used by humanitarian agencies for the assessment of vulnerability to natural hazards. To increase the number of buildings in the dataset that can be enhanced with multiple vulnerability attributes, it is of great importance that the data sources overlap. Therefore, prior to the data collection process, agreement on the target area is essential. Moreover, open source platforms such as OpenAerialMap, Mapillary and OSM can be used to investigate the existing overlap between datasets. This overlap can be used to get insight in the data coverage of target areas. Additionally, new data collection activities can be executed if supplementary data is required.

To increase the accuracy of the output data, it can be considered to use other building footprint data instead of the OSM dataset. The building footprint of OSM is based on satellite data, which in many cases is relatively older. Moreover, the most vulnerable buildings (e.g. with thatched rooftops) are difficult to identify due to the coarser spatial resolution of satellite data. Therefore, in order to obtain better results, future research should focus on the development of accurate building footprint maps, e.g. by using UAV data as a base.

7.3.3 Governmental agencies

One of the most important challenges for up-scaling to other areas is the availability of spatial data. To overcome this problem, it is crucial that spatial datasets, collected by either individuals, humanitarians or governmental agencies, can be openly accessed by everyone from a single portal. Although recent efforts have been made to establish a National Spatial Data Infrastructure (NSDI), Malawi faces several constraints in the actual development. In a study by Mwange et al. (2018), the status of Malawi's SDI was investigated. The major challenges that Malawi faces include inadequate funding, lack of human resource capacity and legal constraints.

It is important for governmental agencies to recognise the benefits of reusable open data. Research should therefore focus on cost-benefit analyses with regard to open data. Moreover, the institutional and legal constraints in the development of the NSDI should be further investigated.

References

Adu, D. T., Kuwornu, J. K., Anim-Somuah, H., & Sasaki, N. (2018). Application of livelihood vulnerability index in assessing smallholder maize farming households' vulnerability to climate change in Brong-Ahafo region of Ghana. *Kasetsart Journal of Social Sciences*, *39*(1), 22–32.

Birkmann, J. (2006). Measuring vulnerability to promote disaster-resilient societies: Conceptual frameworks and definitions. *Measuring vulnerability to natural hazards : Towards disaster resilient societies* (pp. 9–55). United Nations University Press.

Blanco-Vogt, A., Haala, N., & Schanze, J. (2013). Building extraction from remote sensing data for parameterising a building typology: A contribution to flood vulnerability assessment. *Joint Urban Remote Sensing Event 2013, JURSE 2013*, (June 2014), 147–150.

Blaschke, T. (2010). ISPRS Journal of Photogrammetry and Remote Sensing Object based image analysis for remote sensing. *ISPRS Journal of Photogrammetry and Remote Sensing*, *65*, 2–16.

Bryman, A. (2012). *Social research methods* (4th editio). Oxford University Press.

Bucherie, A. (2019). *On the predictability of flash floods and their impacts in North Malawi* (Doctoral dissertation). IHE Delft Institute for Water Education, Delft, the Netherlands.

Bureau TNM. (2016). *Safer House Construction Guidelines - Technical manual* (tech. rep.). https://www.sheltercluster.org/sites/default/files/docs/mlhud-malawi_safer-house-guidelines.pdf

Cao, R., Zhu, J., Tu, W., Li, Q., Cao, J., Liu, B., Zhang, Q., & Qiu, G. (2018). Integrating aerial and street view images for urban land use classification. *Remote Sensing*, *10*(10), 1–23.

CIESIN. (2020). Data Release Statement GRID3 Malawi Settlement Extents Version 01 Alpha. https://data.humdata.org/dataset/grid3-malawi-settlement-extents-version-01-alpha

De Angeli, S., Dell'Acqua, F., & Trasforini, E. (2016). Application of an Earth-Observation-based building exposure mapping tool for flood damage assessment. *3rd European Conference on Flood Risk Management*, 1–13.

De Perez, E. C. (2018). *Forecast-based financing: a scientific foundation for systematic early action* (Doctoral dissertation). Vrije Universiteit Amsterdam.

De Perez, E. C., Van Den Hurk, B., Van Aalst, M. K., Amuron, I., Bamanya, D., Hauser, T., Jongma, B., Lopez, A., Mason, S., De Suarez, J. M., Pappenberger, F., Rueth, A., Stephens, E., Suarez, P., Wagemaker, J., & Zsoter, E. (2016). Action-based flood forecasting for triggering humanitarian action. *Hydrology and Earth System Sciences*, *20*(9), 3549–3560.

de Moel, H., Jongman, B., Kreibich, H., Merz, B., Penning-Rowsell, E., & Ward, P. J. (2015). Flood risk assessments at different spatial scales. *Mitigation and Adaptation Strategies for Global Change*, *20*(6), 865–890.

Ebert, A., Kerle, N., & Stein, A. (2009). Urban social vulnerability assessment with physical proxies and spatial metrics derived from air-and spaceborne imagery and GIS data. *Nat Hazards*, *48*, 275–294.

Englhardt, J., De Moel, H., Huyck, C. K., De Ruiter, M. C., Aerts, J. C., & Ward, P. J. (2019). Enhancement of large-scale flood risk assessments using building-material-based vulnerability curves for an object-based approach in urban and rural areas. *Natural Hazards and Earth System Sciences*, *19*(8), 1703–1722.

Grippa, T., Lennert, M., Beaumont, B., Vanhuysse, S., Grippa, T., Lennert, M., Beaumont, B., Vanhuysse, S., Stephenne, N., & Wolff, E. (2016). An open-source semi-automated processing chain for urban OBIA classification. *Proceedings of the GEOBIA 2016 Conference: Mach-2: Machine Learning & Automation II*, 1–6.

Guillard-Gonçalves, C., & Zêzere, J. L. (2018). Combining social vulnerability and physical vulnerability to analyse landslide risk at the municipal scale. *Geosciences (Switzerland)*, *8*(8).

Hoffmann, E. J., Wang, Y., Werner, M., Kang, J., & Zhu, X. X. (2019). Model fusion for building type classification from aerial and street view images. *Remote Sensing*, *11*(11), 1–20.

IFRC. (2020). ABOUT – Forecast-based Financing. https://www.forecast-based-financing.org/about/

IPCC. (2012). Determinants of risk: Exposure and vulnerability. *Managing the Risks of Extreme Events and Disasters to Advance Climate Change Adaptation: Special Report of the Intergovernmental Panel on Climate Change*, *9781107025*, 65–108.

Kellermann, P., Schröter, K., Thieken, A., Haubrock, S.-N., & Kreibich, H. (2020). The object-specific flood damage database HOWAS21. *Natural Hazards and Earth System Sciences*, *20*(September), 2503–2519.

Khalfan, M. (2013). *Fragility curves for residential buildings in developing countries: A case study on non-engineered URM homes in Bantul, Indonesia* (Doctoral dissertation). McMaster University, Hamilton, Ontario, Canada.

Kienberger, S. (2012). Spatial modelling of social and economic vulnerability to floods at the district level in Búzi, Mozambique. *Natural Hazards*, *64*(3), 2001–2019.

Kienberger, S., Blaschke, T., & Zaidi, R. Z. (2013). A framework for spatio-temporal scales and concepts from different disciplines: The 'vulnerability cube'. *Natural Hazards*, *68*(3), 1343–1369.

Kloukinas, P., Novelli, V., Kafodya, I., Ngoma, I., Macdonald, J., & Goda, K. (2020). *A building classification scheme of housing stock in Malawi for earthquake risk assessment* (Vol. 35). Springer Netherlands.

Lang, S., Kienberger, S., Tiede, D., Hagenlocher, M., & Pernkopf, L. (2014). Geons-domain-specific regionalization of space. *Cartography and Geographic Information Science*, *41*(3), 214–226.

Loos, S., Lallemant, D., Baker, J., McCaughey, J., Yun, S. H., Budhathoki, N., Khan, F., & Singh, R. (2020). G-DIF: A geospatial data integration framework to rapidly estimate post-earthquake damage. *Earthquake Spectra*, *36*(4), 1695–1718.

Malawi Government. (2015). *Flood Risk Modelling for the North and Central Malawi* (tech. rep.). https://www.preventionweb.net/publications/view/54387

Malawi Government. (2019). *Malawi 2019 Floods Post Disaster Needs Assessment Report Malawi Government* (tech. rep.).

Mapillary. (2019). Object detections – Mapillary. https://help.mapillary.com/hc/en-us/articles/115000967191-Object-detections

Merz, B., Aerts, J., Arnbjerg-Nielsen, K., Baldi, M., Becker, A., Bichet, A., Blöschl, G., Bouwer, L. M., Brauer, A., Cioffi, F., Delgado, J. M., Gocht, M., Guzzetti, F., Harrigan, S., Hirschboeck, K., Kilsby, C., Kron, W., Kwon, H. H., Lall, U., ... Nied, M. (2014). Floods and climate: Emerging perspectives for flood risk assessment and management. *Natural Hazards and Earth System Sciences*, *14*(7), 1921–1942.

Merz, B., Kreibich, H., Schwarze, R., & Thieken, A. (2010). Review article "Assessment of economic flood damage". *Natural Hazards and Earth System Sciences (NHESS)*, *10*, 1697–1724.

Merz, B., Thieken, A. H., & Gocht, M. (2007). Flood Risk Mapping at the Local Scale: Concepts and Challenges. *Flood risk management in europe* (pp. 231–251). Springer.

Mwange, C., Mulaku, G. C., & Siriba, D. N. (2018). Reviewing the status of national spatial data infrastructures in Africa. *Survey Review*, *50*(360), 191–200.

Nasiri, H., Mohd Yusof, M. J., & Mohammad Ali, T. A. (2016). An overview to flood vulnerability assessment methods. *Sustainable Water Resources Management*, *2*(3), 331–336.

OECD. (2008). *Handbook on Constructing Composite Indicators: Methodology and User Guide*. OECD Publishing.

Papathoma-Köhle, M. (2016). Vulnerability curves vs. Vulnerability indicators: Application of an indicator-based methodology for debris-flow hazards. *Natural Hazards and Earth System Sciences*, *16*(8), 1771–1790.

Qian, Y., Zhou, W., Yan, J., Li, W., & Han, L. (2015). Comparing machine learning classifiers for object-based land cover classification using very high resolution imagery. *Remote Sensing*, *7*(1), 153–168.

Reinoso, E., Ordaz, M., Cardona, O. D., Bernal, G. A., Cardona, O.-D., Bernal, G. A., & Contreras, M. (2018). *AFTER 10 YEARS OF CAPRA* (tech. rep.). https://www.researchgate.net/publication/326274673

Rudari, R., Beckers, J., De Angeli, S., Rossi, L., & Trasforini, E. (2016). Impact of modelling scale on probabilistic flood risk assessment: the Malawi case. *FLOODrisk 2016 - 3rd European Conference on Flood Risk Management DOI:* 1–12.

Schneiderbauer, S., & Ehrlich, D. (2006). Social levels and hazard (in)dependence in determining vulnerability. *Measuring vulnerability to natural hazards : Towards disaster resilient societies, by birkmann, j.* (pp. 78–103). United Nations University Press.

Shelter cluster. (2015). Key Shelter Safety Messages- 2015 Malawi Floods and Storms. https://www.sheltercluster.org/sites/default/files/docs/key_messages_2015_malawi_floods_and_storms.pdf

Tarbotton, C., Dall'Osso, F., Dominey-Howes, D., & Goff, J. (2015). The use of empirical vulnerability functions to assess the response of buildings to tsunami impact: Comparative review and summary of best practice. *Earth-Science Reviews*, *142*, 120–134.

UNDRR. (2019). *Global Assessment Report on Disaster Risk Reduction* (tech. rep.). United Nations. Geneva.

UN-HABITAT. (2010). *Malawi Urban Housing Sector Profile* (tech. rep.). United Nations Human Settlements Programme (UN-HABITAT). Nairobi, Kenya. https://unhabitat.org/malawi-urban-housing-sector-profile

UNISDR. (2017). Flood hazard and risk assessment. (September), 12–23.

VCA. (2020). *VCA REPORT-Strengthening Resilience in Malawi, Karonga* (tech. rep.). ECHO. https://gis-malawi.com/resources/pdf/Karonga%20ECHO%20STRIM%20eVCA%20Report.pdf

Wilkinson, E., Weingärtner, L., Choularton, R., Bailey, M., Todd, M., Kniveton, D., & Cabot Venton, C. (2018). *Forecasting hazards, averting disasters Implementing forecast-based early action at scale* (tech. rep.). www.odi.org/twitter

World Resource Institute. (2020). RELEASE: New Data Shows Millions of People, Trillions in Property at Risk from Flooding — But Infrastructure Investments Now Can Significantly Lower Flood Risk — World Resources Institute. https://www.wri.org/news/2020/04/release-new-data-shows-millions-people-trillions-property-risk-flooding-infrastructure

Wouters, L., Moel, H. d., Ruiter, M. d., Couasnon, A., Homberg, M. v. d., Teklesadik, A., & Margutti, J. (2020). Improving flood damage assessments in data-scarce areas by retrieving building characteristics through automated UAV image processing.

Wright, D. B. (2015). Methods in Flood Hazard and Risk Assessment. https://openknowledge.worldbank.org/bitstream/handle/10986/22982/Methods0in0flo00and0risk0assessment.pdf?sequence=1

Wu, J., & Li, H. (2006). Concepts of scale and scaling. *In: Wu j., jones, k.b., li. h, loucks, o. l., scaling and uncertainty analysis in ecology: Methods and applications* (pp. 1–351).

8 Appendix

Appendix A: OBIA Validation

	P	R	F-1
Bare	0,6	0,23	0,33
Iron	0,81	0,62	0,7
Shadow	0,93	0,81	0,87
Thatch	0,625	0,84	0,72
Vegetation	0,96	0,99	0,98
Road	0,86	0,82	0,84

Table 19: Class performance of the OBIA model

		Actual					
		Bare soil	**Iron**	**Shadow**	**Thatch**	**Vegetation**	**Road**
Predicted	**Bare soil**	9	0	0	30	0	0
	Iron	1	79	0	41	4	3
	Shadow	0	0	26	4	2	0
	Thatch	4	15	2	125	2	0
	Vegetation	1	0	0	0	183	0
	Road	0	4	0	0	0	19

Table 20: Confusion matrix OBIA model

Appendix B: Summary ECHO 3 survey results

In the ECHO 3 survey, 32,7% of the buildings have thatched rooftops and 64,9% iron rooftops. The majority of the buildings with thatched rooftops have type 1 wall materials (mud, bamboo, poles). The majority of the buildings with iron rooftops have walls made of burnt bricks.

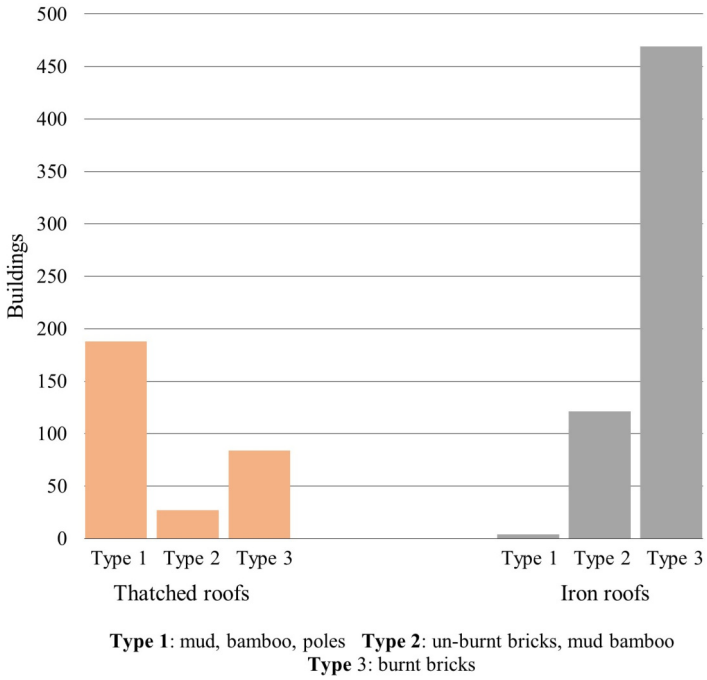

Figure 26: The distribution of wall material in Karonga, based on ECHO 3 data

The households survey shows that of the 915 households that participated, 10% of the houses belong to the permanent building class, 67,9% is semi-permanent and 22,1% is temporary.

Building type	Percentage	Number
Traditional	22,1%	202
Semi-permanent	67,9%	621
Permanent	10%	92

Table 21: Distribution of building types in Karonga, based on ECHO 3 data